EFFECT OF ROD GAP SPACING ON A SUCTION PANEL FOR LAMINAR FLOW AND NOISE CONTROL IN SUPERSONIC WIND TUNNELS

by

William D. Harvey

A thesis presented in partial fulfillment
of the requirements for the Degree of

MASTER OF ENGINEERING

in

Mechanical Engineering
Old Dominion University
May 1975

Supervisory Committee

Dr. Robert Ash (Thesis Advisor)

I. E. Beckwith (NASA)

Dr. Gene Goglia (ODU)

Old Dominion University
School of Engineering

ABSTRACT

EFFECT OF ROD GAP SPACING ON A SUCTION PANEL FOR LAMINAR FLOW AND NOISE CONTROL IN SUPERSONIC WIND TUNNELS

By

William D. Harvey

Advisors: Dr. Robert L. Ash (ODU) and I. E. Beckwith (NASA)

May 1975
Norfolk, Virginia 23508

ABSTRACT

It has been well established that the test section flow of conventional supersonic and hypersonic wind tunnels contains significant levels of disturbances. These disturbances are mainly caused by the radiation of aerodynamic noise from the turbulent boundary layer on the nozzle walls. This noise level has been shown to have an important effect on boundary layer transition measured on models in tunnels. The purpose of this thesis is to present results of a coordinated experimental and theoretical study of a sound shield concept which aims to provide a means of noise reduction in the test section of supersonic wind tunnels at high Reynolds numbers. The model used in the investigation consists of a planar array of circular rods aligned with the flow, with adjustable gaps between them for boundary layer removal by suction, i.e., laminar flow control. One of the basic requirements of the present sound shield concept is to achieve sonic cross flow through the gaps in order to prevent lee-side flow disturbances from penetrating back into the shielded region. Tests have been conducted at Mach 6 over a local unit Reynolds number range from about 1.2×10^6 to 13.5×10^6 per foot. Measurements of heat transfer, static pressure, and sound levels are made to establish the transition characteristics of the boundary layer on the rod array and the sound shielding effectiveness.

For a gap-to-rod diameter ratio of 0.16, the flow is laminar over the entire model at a maximum local Reynolds number based on model length of about 15×10^6 which occurs at a unit Reynolds number of about 7.5×10^6 per foot. At this unit Reynolds number the transition Reynolds number on a conventional flat plate in the same wind tunnel is 2×10^6. Transition Reynolds number on the suction model decreases with decreasing gap spacing and suction but the model still provides a significant increase in transition Reynolds number over that for a flat plate. The characteristics of the boundary layer flow on the rods and the transition behavior indicates that for large gaps the circular rods function as isolated swept cylinders. Hence, transition is expected to be essentially independent of rod length and therefore should be primarily a function of Reynolds number based on rod diameter for a given gap spacing and leading edge configuration.

For a gap-to-rod diameter ratio of 0.16, reduction in sound levels within the semi-shielded region of the model were about 90 percent (20 dB attenuation) of the maximum theoretical reduction for an ideal, finite, planar shield. Reductions in gap spacing and suction caused reductions in the sound attenuation. It is concluded that a cylindrical shroud utilizing the slotted wall concept with boundary layer suction can provide significant reductions of disturbance levels in supersonic wind tunnels at high unit Reynolds numbers.

TABLE OF CONTENTS

ACKNOWLEDGEMENTS

The author would like to extend his appreciation to Ivan E. Beckwith and Dennis M. Bushnell, NASA-Langley, for their continued interest and support during this investigation. Their experience and suggestions have enhanced the author's knowledge regarding this study. I would like to thank Dr. Robert L. Ash for his interest as my advisor and help in this thesis preparation. Also, I would like to thank Dr. Gene Goglia and Dr. A. S. Roberts of the Mechanical Engineering Department of Old Dominion University for their assistance in the graduate program. Finally, I would like to thank my wife for her cooperation during this graduate program.

LIST OF FIGURES

FIGURE

SYMBOLS

C_p	Specific heat
D	Rod diameter
G	Width of minimum gaps between rods
$G^* =$	$G - 2\delta^*$
h	Heat transfer coefficient, $\dot{q}/(T_{aw} - T_w)$
ℓ	Mixing length
M	Mach number
p	Pressure
Pr	Prandtl number
P_t'	Normalized ratio of rms pitot pressures $(\tilde{p}_t/\overline{p}_t)_\infty$ / $(\tilde{p}_t/\overline{p}_t)_{\bar{\infty}}$
p_t	Pitot pressure
Q	Magnitude of resultant velocity vector
$\dot{q}$	Local heat-transfer rate Btu/ft^2-sec
Re/ft	Local unit Reynolds number, $\left(\frac{w}{\nu}\right)_\infty$
$Re_{,x}$	Length Reynolds number based on x distance, $\left(\frac{w}{\nu}\right)_\infty x$
r	Recovery factor
St	Stanton number, $\dot{q}/\rho_\infty C_p Q_\infty (T_{aw} - T_w)$
T	Absolute temperature, ^oR
t	Thickness
u	Chordwise velocity component
w	Spanwise velocity component
x	Distance from model leading edge

y	Distance normal to surface
α	Angle of attack
α_{eff}	Local effective angle of attack
β	Local effective sweep angle, $90^{o} - \alpha_{eff}$
γ	Ratio of specific heats, 1.4 used throughout
θ	Shock angle
τ	Time
ν	Kinematic viscosity, μ/ρ
ϕ	Chordwise angle measured from stagnation line of circular rods
ω	Local flow turning angle with respect to rod stagnation line

Subscripts

aw	Adiabatic wall
B	Bottom of rod surface (leeside)
D	Based on rod diameter
G	Gap
$s\ell$	Inviscid flow at stagnation line
T	Top of rod surface (windward side)
t	Transition
w	Wall or surface
o	Settling chamber conditions
$\bar{\infty}$	Test section free stream
∞	Rod model flow field far from the rods

1	Behind normal shock
2	In front of normal shock or total conditions

Superscripts

$(\bar{})$	Time mean value
$(\tilde{})$	rms fluctuating value

I. INTRODUCTION

Extensive research conducted in the area of boundary layer transition has of necessity been carried out in wind tunnels, there being no practical way at present of making detailed experimental measurements in free flight. Transition phenomena investigated in wind tunnels have too often been inconsistent and unexplainable. An informative evaluation of the high-speed transition problem in wind tunnels and free flight has been presented by Morkovin [1].*

As is now well known, the test section flow of conventional supersonic and hypersonic wind tunnels are noisy. Laufer [2] proposed and later showed [3] that sound disturbances observed in the test section were caused by the radiation of aerodynamic noise from the turbulent boundary layer on the walls of tunnels. This noise (pressure fluctuations) has an important effect on transition measured on test models in wind tunnels [3-9]. For example, the transition Reynolds number has been shown by Stainback et al. [6] to vary inversly with tunnel rms pressure disturbance levels which range from about 1 to 5 percent of the free stream static pressure. In addition, wind tunnel noise was believed to cause premature transition on swept wings with suction for laminar flow control [10]. Other measurements made in wind tunnels that might be influenced by noise in the test section are the mixing rates in free shear layers, stagnation point heating rates to blunt bodies, and the properties of laminar and turbulent boundary

* The number in the brackets indicate references.

layers on models. Beckwith [11] has demonstrated that, for turbulent flow, the validity of Crocco's solution to the energy equation is subject to the requirement of small pressure fluctuation levels.

A wind tunnel with reduced disturbance levels (a "quiet" tunnel -- having laminar rather than turbulent boundary layers on the facility walls) is required to conduct valid research in these areas. Several concepts currently being considered or undergoing development for use in such a quiet tunnel have been discussed by Beckwith [12]. Recent encouraging experimental data [13] showed that laminar boundary layers can be maintained on the walls of a conventional nozzle at larger Reynolds numbers than previously reported, merely by polishing the surface and heating the nozzle wall. The test section disturbance levels were reduced by about an order of magnitude. Results obtained in a nozzle with boundary layer bleed upstream of the sonic throat showed that transition in the boundary layer on the nozzle wall occurred at higher Reynolds numbers than for conventional nozzles [13]. However, at higher operating unit Reynolds numbers the boundary layer on the wall becomes turbulent and other devices for the suppression and control of noise are required for meaningful transition testing. The purpose of this thesis is to report on an investigation of a sound shield concept.

1.1 Laminar Flow Control and Sound Shield Research

Pate and Schueler [9] have shown that free stream rms pressure fluctuations at Mach 3 were reduced by 40 to 50 percent within a region shielded by a solid wall cylindrical shroud provided the boundary layer

on the inside wall of the shroud was laminar. The dominant mechanism accounting for the residual noise level within the shielded region was probably reflection of sound from the inside walls of the shroud. However, convection of sound directly into the shielded region by the flow and transmission through the walls of the shroud may also have contributed to the residual noise to some extent. Thus a shroud appears to offer a way to shield a test area from radiated noise and reduce the free stream disturbances at high operating pressures if a method can be developed to prevent the boundary layer on the inside of the shield from becoming turbulent.

Earlier considerations have been given to the use of both slotted and porous walls with suction for maintaining laminar boundary layers on tunnel walls for noise reduction. Pfenninger and Syberg [14] have recently conducted an extensive study of suction through porous walls in wind tunnels to laminarize the nozzle wall boundary layer for the reduction of acoustic disturbances in the test section at supersonic and hypersonic speeds. Supersonic laminar boundary layers have been maintained for Reynolds numbers up to 51×10^6 by using spanwise slots [15], however, disturbances were present in the flow due to the disturbances at the slots. Klebanoff and Spangenberg [16] at the National Bureau of Standards have maintained laminar boundary layers on nozzle walls up to Reynolds numbers of about 3.5×10^6 by using longitudinal rods with suction in a Mach 2 wind tunnel. A concept similar to that of Klebanoff and Spangenberg has been tested at the NASA Langley Research Center. Preliminary results with a flat sound shield

model constructed with longitudinal rods (rods aligned with the flow) indicated that transition could be delayed to higher Reynolds numbers than on a conventional flat plate while the noise levels measured in the shielded region were reduced by about 30 to 40 percent from the free stream level [16]. Harvey et al. [17] reported on an experimental and theoretical analysis of an improved flat rod model for laminar flow and noise control in supersonic wind tunnels.

A recent investigation has been conducted from subsonic to supersonic speeds by Binion and Anderson [18] using a slotted test section wall configuration composed of longitudinal rods similar to the present model but without forced suction to evaluate the effectiveness of this rod wall for reducing transonic wind tunnel disturbances. They concluded that, while the rod walls are no panacea for two-dimensional transonic wall interference problems, results indicated that further work on rod wall concepts merit consideration during development of the next generation of transonic wind tunnels.

This brief analysis of previous techniques for maintaining laminar flow to high Reynolds numbers and the potential of a shroud to shield a test region from radiated noise suggest that some type of sound shield or shroud attenuation device could be used to reduce and control test section disturbances in supersonic wind tunnels. This shield should be designed to minimize self-generated disturbances by boundary layer bleed at the suction surface.

1.2 Sound Shield Concept

A complete analysis and understanding of the acoustic characteristics of the present sound shield concept is considered beyond the scope of this thesis. However, it is possible to establish general principles of sound shielding. The requirements for efficient operation of sound radiation shielding for the present purposes are illustrated in Figure 1.1. Weak pressure disturbances in a supersonic flow travel along Mach waves, so noise from the turbulent boundary layer on the top wall of the nozzle is radiated directly into the "half-shielded" region of the model. Some of this incident sound field is reflected and transmitted by the rods and absorbed through the gaps. The model is operated at angle of attack to establish a pressure drop across the rod array. If this pressure drop is large enough sonic cross flow occurs in the gaps of the rod array and prevents lee-side disturbances from entering the shielded region.

It is well known that sound radiated by a turbulent boundary layer is much greater than that for a laminar boundary layer. Therefore, it is necessary to maintain laminar flow over the rod array by the use of suction for boundary layer removal. Test models placed within the shielded region (Figure 1.1) would be partially shielded from noise radiated from the nozzle wall boundary layer. The objectives of the rod sound shield research was to optimize the design in order to promote the maintenance of a laminar boundary layer and reduce free stream disturbances.

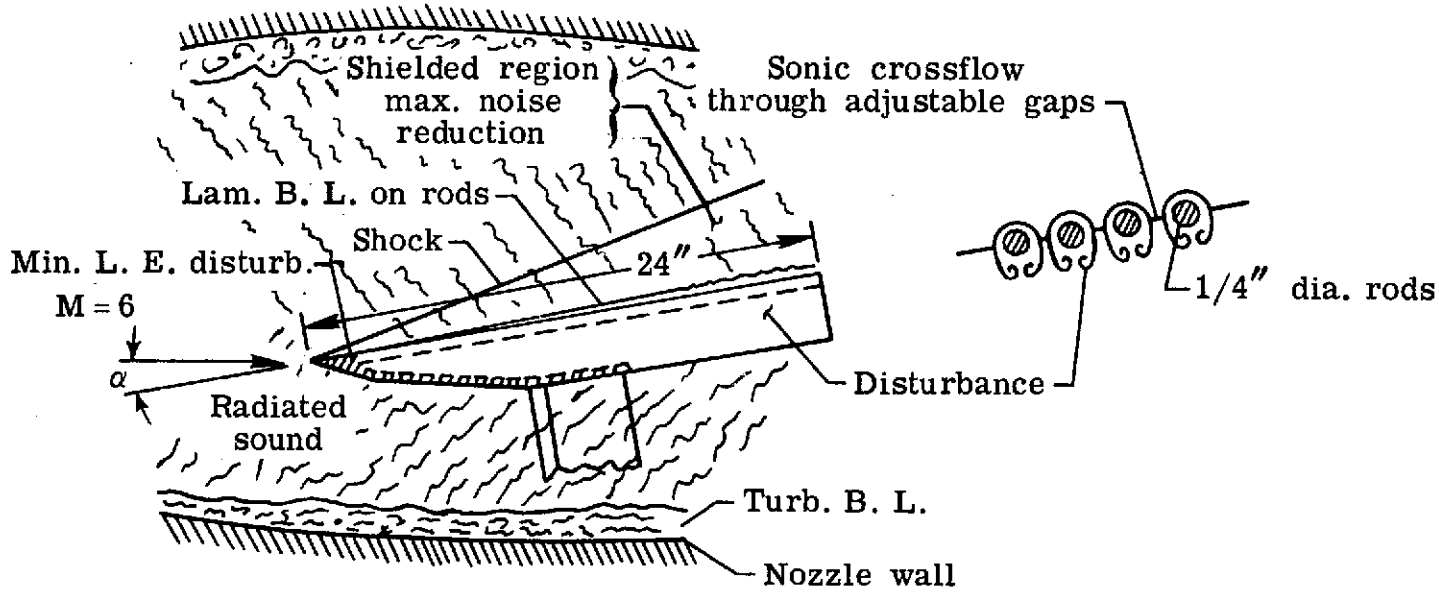

Figure 1.1.- Sketch illustrating principle of shielding concept for laminar flow suction model.

II. MODEL DESCRIPTION

Photographs of the noise shield model used during the present experimental investigation are shown in Figure 2.1. A sketch of the model is shown in Figure 2.1.1 which illustrates important construction features. This model was chosen for the present proof of concept tests to simplify construction and operational techniques. The model consisted of a planar array of circular rods aligned parallel to the flow. The rods were faired into a sharp flat plate at the leading edge. Gaps were provided between the rods for boundary layer removal and the width of the gaps was adjustable to control the suction mass flow rate through the gaps. The rods were supported by the flat plate leading edge and three cross support members perpendicular to the rods. The two central rod support stringers shown in Figure 2.1.1 are 0.125-inch diameter rods. The transverse support at the rear of the model is 0.50-inch in diameter. The bottom of the model is covered with a solid plate (cross hatched area in Figure 2.1.1) over the forward half of the model to maintain the lee-side region of the rods at base pressure when the model is placed at angle of attack.

The upper sketch in Figure 2.1.1 shows a top view of the leading edge and rod junctions. The circular rods have a flat-to-round shaped fairing region downstream of their junction with the flat plate leading edge. Spacers (Figure 2.1.1) are placed between the rods in this forward region and at the rear transverse support to set the desired width of the

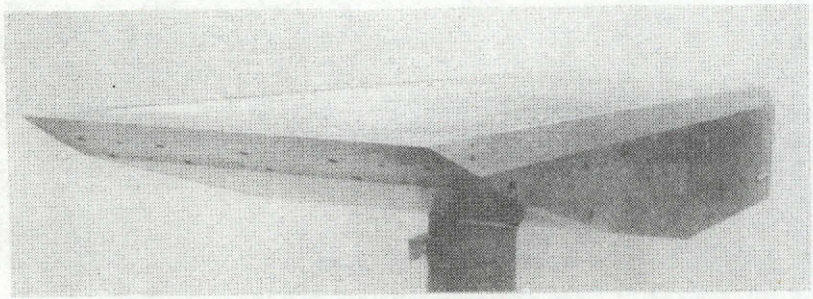

FRONT AND SIDE VIEW

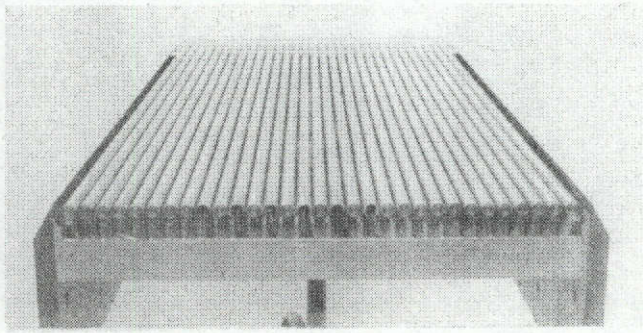

REAR VIEW

Figure 2.1.- Laminar flow suction model.

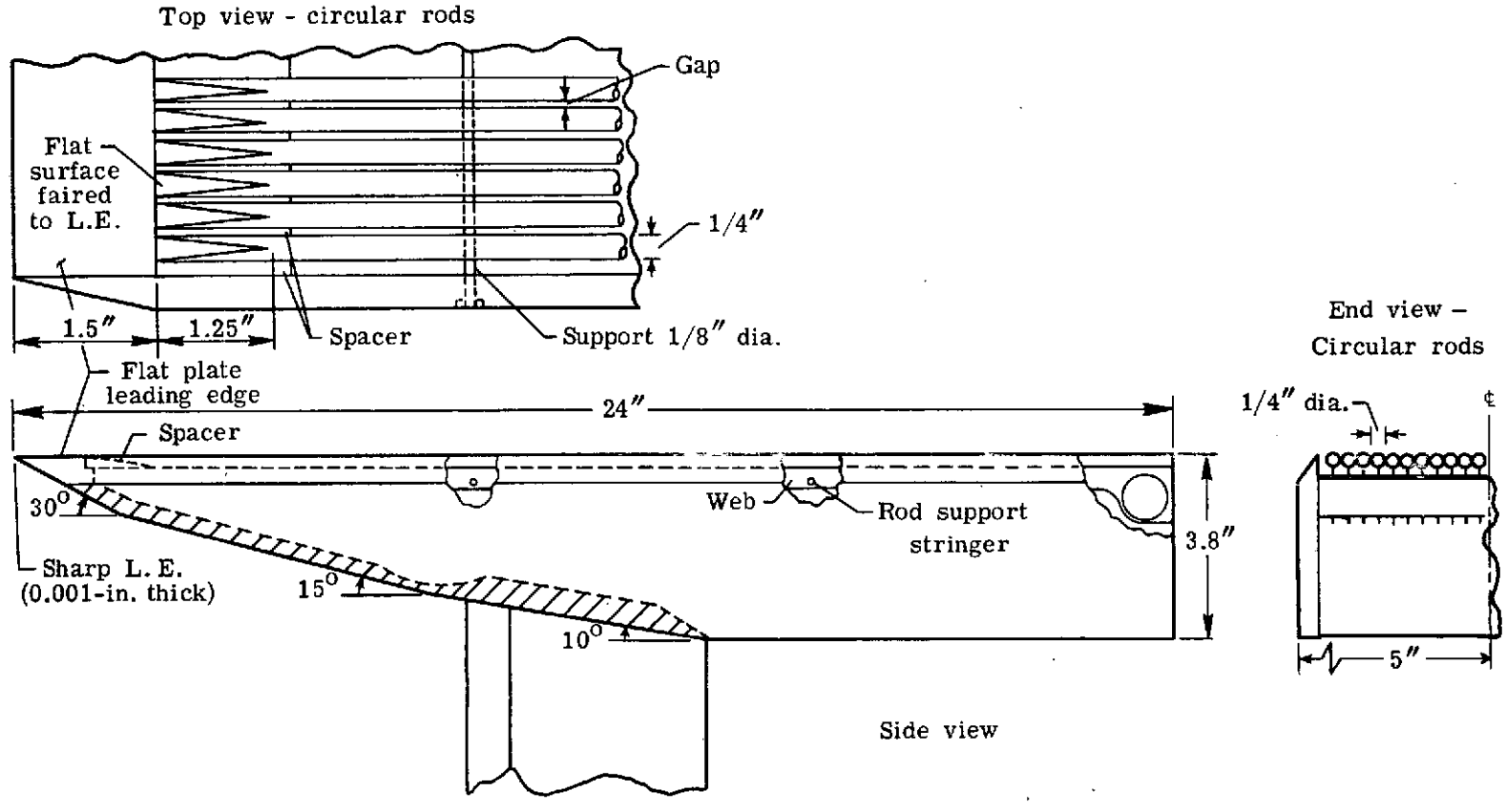

Figure 2.1.1.- Sketch of flat plate rod model.

gaps at these stations. The support stringers were threaded and small nuts were then set on each side of the webs to maintain the correct gap spacing along the entire length of the rods. The model was tested at angle of attack to produce a pressure ratio across the rods that was usually sufficient to insure sonic cross flow in the gaps.

Two hollow-rods, with wall thickness of 0.028-inch, were instrumented with 21 thermocouples spaced evenly along their length and located on the windward stagnation line. The standard transient technique [19] to measure the heating rates was used. Four rods have pressure orifices located at chordwise stations of $\phi = 0^{o}$, 90^{o}, and 180^{o} at several longitudinal stations.

III. INSTRUMENTATION

Chromel-alumel wires of 0.005-inch diameter were spot-welded to the inside surface of the thin wall hollow rods to form the thermocouple junctions. The wire leads were brought out at the model rear through the inside of the hollow rods.

The pressure orifices were 0.040-inch diameter. The pressure tube lengths were kept at a minimum of about six feet to reduce lag. Capacitance type pressure transducers were used that had a range selection feature which provided seven ranges with fullscale readout on each range. Either automatic or manual range change selection was available. The accuracy of all pressure transducer readings was 0.25 percent of fullscale reading.

Pressure data acquisition was continuously monitored during each test until the readings were constant.

IV. TEST CONDITIONS

The rod model was tested in the Langley Mach 6, 20-Inch Tunnel with air as the test medium. Tests were conducted at 5^{o} and 10^{o} angle of attack for gap-to-diameter ratios of G/D = 0.068, 0.12, and 0.16. The local unit Reynolds number range for these tests was about $1.2 \times 10^{6} \leq$ Re/ft $\leq 13.5 \times 10^{6}$ for $T_w/T_o \simeq 0.63$. Free stream disturbance levels in the tunnel test section have been measured over a range of unit Reynolds number [6].

V. THEORY

An analysis of the inviscid and boundary layer flow on the rods for the present model has previously been made by Berger [20] using the computer program of Reference [21] for infinite swept cylinders. Laminar and turbulent predictions [20] of the local Stanton numbers on the windward side of the rods have previously been made and compared to experimental data [17,20] for G/D = 0.16 at Mach 6. Laminar predictions for values of G/D < 0.16 were also made [20] with some participation from this author and are shown herein compared to data.

Infinite swept cylinder concepts are applied to the flow on the rods in the region downstream of the flat plate leading edge-rod junctions (Figure 2.1.1) [20]. In the analysis by Berger [20], one of the inputs to

the boundary layer program [21] was the local effective angle of attack α_{eff}, that yields very large sweep angles for the circular rods. In view of the large effective sweep angles of the present rods with respect to the local flow ($\simeq 89^{o}$), the boundary layer behavior was surprisingly well represented by swept cylinder theory [17, 20] for G/D = 0.16 at Mach 6. Following the analysis by Berger [20], the cross flow normal to the rods is considered independent of the streamwise flow but dependent on the suction mass flow area. Thus, from continuity, the ratio of chordwise-to-spanwise velocity in the local free stream is (see Figure 5.1):

$$\frac{u_\infty}{w_\infty} = \frac{(\rho u)_G}{(\rho w)_\infty} \quad \frac{G^*}{(D+G)} \tag{1}$$

From the perfect gas law and definition of the speed of sound, equation (1) may be expressed as follows

$$\frac{u_\infty}{w_\infty} = \frac{p_G}{p_\infty} \left(\frac{T_\infty}{T_G} \right)^{1/2} \quad \frac{(M)_{u,G}}{(M)_{w,\infty}} \quad \frac{G^*}{(D+G)} \tag{2}$$

In terms of the stagnation line conditions on the rods and for sonic gap flow $(M)_{u,G} = 1.0$, equation (2) may be expressed as

$$\frac{u_\infty}{w_\infty} = \frac{p_G}{p_{s\ell}} \quad \frac{p_{s\ell}}{p_\infty} \quad \left(\frac{T_\infty}{T_{s\ell}} \quad \frac{T_{s\ell}}{T_G} \right)^{1/2} \quad \frac{1}{(M)_{w,\infty}} \quad \frac{G^*/D}{1 + G/D} \tag{3}$$

Since $(M)_{w,\infty} = (M)_{Q,\infty} \cos \alpha_{eff}$ and for sonic flow at the gap

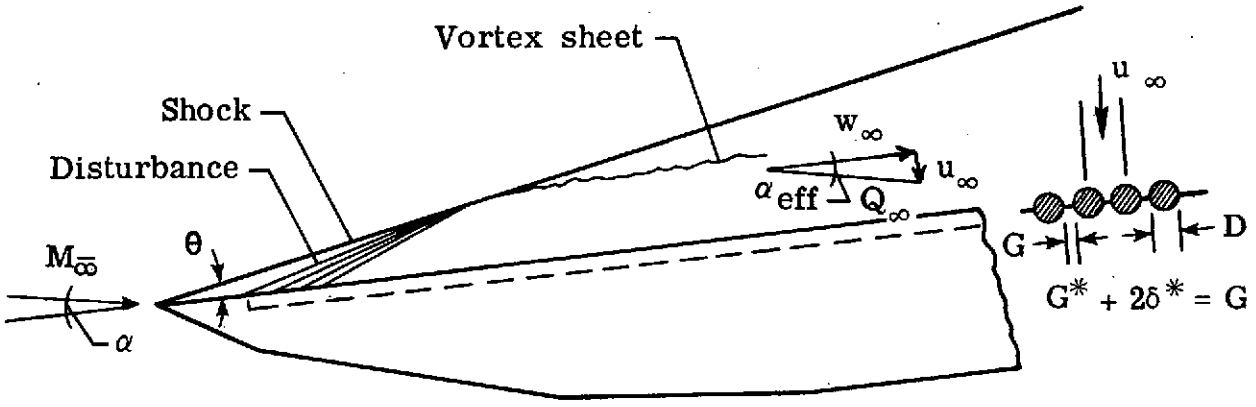

Figure 5.1.- Sketch of rod model flow field and local free stream conditions.

$$\frac{p_G}{p_{s\ell}} = 0.5283 \qquad \text{and} \qquad \frac{T_G}{T_{s\ell}} = 0.8333$$

equation (3) may be expressed as

$$\alpha_{eff} = \tan^{-1} \left\{ \frac{0.5787}{\cos \alpha_{eff} (M)_{Q,\infty}} \quad \frac{\sqrt{T_\infty/T_{s\ell}}}{p_\infty/p_{s\ell}} \quad \frac{G^*/D}{1 + G/D} \right\} \qquad (4)$$

From the known free stream conditions ahead of the model, calculation of the local free stream conditions was accomplished by using the conventional wedge relations for crossing the oblique shock attached to the flat plate leading edge followed by a Prandtl-Meyer expansion, α_{eff}, across the disturbance (Fig. 5.1). For typical conditions in the present tests, $\alpha_{eff} \simeq 1^o$, and to a first approximation $G \simeq G^*$, thus resulting in extremely large sweep angles of $\beta \simeq 89^o$. This large value of β becomes an important factor in the present heat transfer calculations since one would expect that swept cylinder heating would approach the conventional flat plate value. For an isolated swept cylinder without induced cross flow, the cross flow velocity would approach zero as β approaches 90^o resulting in a reduction in the heating rate. Further details for the boundary layer inputs are given by Berger [20] along with calculated results on the present model for the chordwise velocity distribution, cross flow stability, viscous, and gap spacing effects.

VI. DATA REDUCTION

Measured heat-transfer rates along the rod windward stagnation line were determined from the general heat-transfer-rate equation for a calorimeter

$$\dot{q}_w = \rho_w \, c_{p,w} \, t_w \, \frac{dT}{d\tau} \tag{5}$$

where ρ_w, $c_{p,w}$, and t_w are based on the rod material and wall thickness. The derivative $dT/d\tau$, was determined from the measured slope of each thermocouple output at discrete time intervals. For the present calculations, the local Stanton number is

$$St = h/\rho_\infty \, Q_\infty \, c_p \tag{6}$$

where

$$h = \dot{q}_w \, / \, (T_{aw} - T_w) \tag{7}$$

and

$$\frac{T_{aw}}{T_o} = r \left(1 - \frac{T_\infty}{T_o} \right) + \frac{T_\infty}{T_o} \tag{8}$$

The recovery factor $r = \sqrt{P_r}$ for laminar flow and $r = \sqrt[3]{P_r}$ for turbulent flow. The derivative $dT/d\tau$ in equation (5) was evaluated during time intervals of less than 10 seconds after injection of the model into the test flow.

VII. RESULTS AND DISCUSSION

7.1 Pressure Data

Detailed pressure measurements around the circular rods at several chordwise stations have previously been made [17] and compared with predictions [17, 20] for several gap-to-diameter ratios over a Reynolds number range at Mach 6 and $\alpha = 10^{0}$. In general, the agreement between data and predictions [17] was good and indicated that sonic cross flow in the gaps was achieved by induced suction for G/D = 0.16 over a wide range of local unit Reynolds numbers at $\alpha = 10^{0}$.

Static pressures on the rods at $\phi = 0^{0}$, 90^{0}, and 180^{0} were also measured in this investigation for G/D = 0.068, 0.12, and 0.16 at distances downstream of the model leading edge of x = 5.5, 12.5, and 19.5-inches over a range of local unit Reynolds number. The ratio of measured static pressure on the windward stagnation line or top of the rods (p_T) to the tunnel settling chamber pressure is shown in Figure 7.1.(a) for these longitudinal stations and gap spacings for $M_\infty = 6$ and $\alpha = 10^{0}$ to illustrate the variation of static pressure along the rods with Re/ft. The pressure varies slightly both with longitudinal distance and Reynolds number for all gap spacings. The data scatter observed for x = 5.5-inches is probably due to the flat plate leading edge-rod junction disturbance produced at $x \simeq 3$-inches (to be discussed later) or the initial development of suction flow in the gaps in this forward region. The trends of the measured pressures with longitudinal distance and Re/ft is similar to that expected on a flat plate without suction and flow separation.

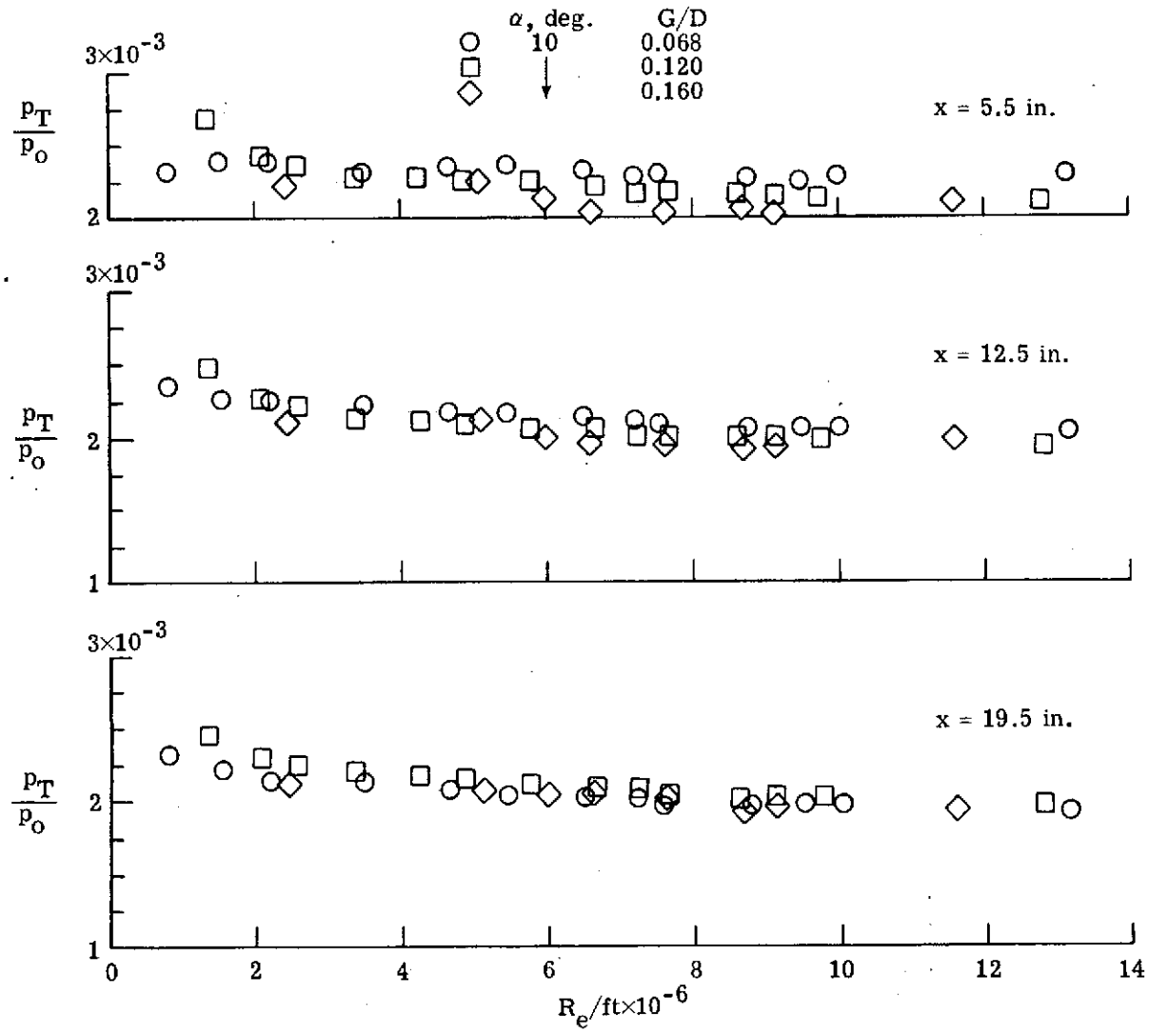

(a) Pressure on windward stagnation line ($\phi = 0^o$)

Figure 7.1.- Comparison of measured static pressure on rod model; $M_\infty = 6$, $T_w = 530^oR$.

The measured values of p_T in Figure 7.1.(a) have been used to normalize the measured values of the pressure at the rod physical gap minimum ($\phi = 90^o$) and rod bottom ($\phi = 180^o$) to determine if sonic cross flow occurred in the gaps. Figures 7.1.(b) and (c) give a summary of the effect of gap spacing on sonic cross flow for the circular rod model over a range of local Reynolds number. Results are shown for G/D = 0.068, 0.12, and 0.16 at $\alpha = 5^o$ and 10^o. The ratio of measured static pressure on the rod side (p_s) to the top (p_s/p_T) and rod bottom pressure (p_B) to the top (p_B/p_T) is shown for several longitudinal stations along the rods. Values of p_B/p_T for all gap spacings and angle of attack are below 0.528 (M = 1) (Fig. 7.1.(c)) indicating that sufficient pressure drop through the rod gaps was present to obtain sonic cross flow. Also, the values of p_B/p_T for $0.068 \leq G/D \leq 0.12$ at $\alpha = 5^o$ are higher than the values for $\alpha = 10^o$ for $Re/ft \geq 4 \times 10^6$. The values of p_s/p_T for G/D = 0.068 at $\alpha = 10^o$ and $0.068 \leq G/D \leq 0.16$ at $\alpha = 5^o$ (Fig. 7.1.(b)) are always above 0.528, possibly because of boundary layer viscous effects. The effective minimum flow area would be expected to change significantly for the lower gap spacings and suction due to boundary layer displacement effects around the rods [20]. This effect would cause a shift in the true or flow gap minimum downstream of the physical minimum where the measurement of p_s/p_T was made. The pressure data at the gap (p_s/p_T) for $Re/ft < 3 \times 10^6$ are higher than the values for $Re/ft > 3 \times 10^6$ for G/D = 0.068 at $\alpha = 10^o$ possibly due to transition of the rod boundary layers as will be discussed later. It is apparent that viscous gap flow effects may have become dominant with reduced G/D and Reynolds number.

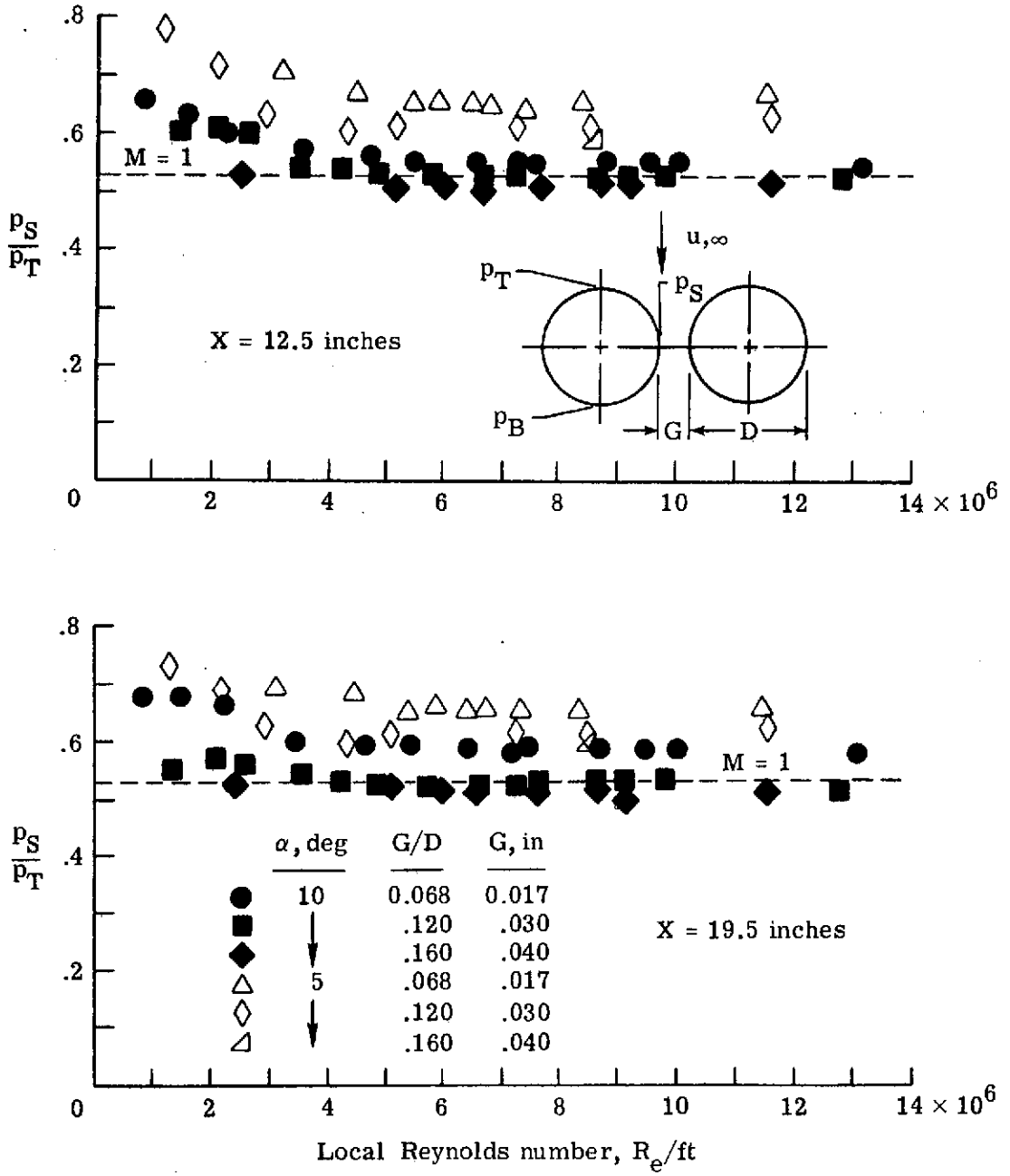

(b) Effect of gap spacing on sonic crossflow at the gap.

Figure 7.1.- Continued.

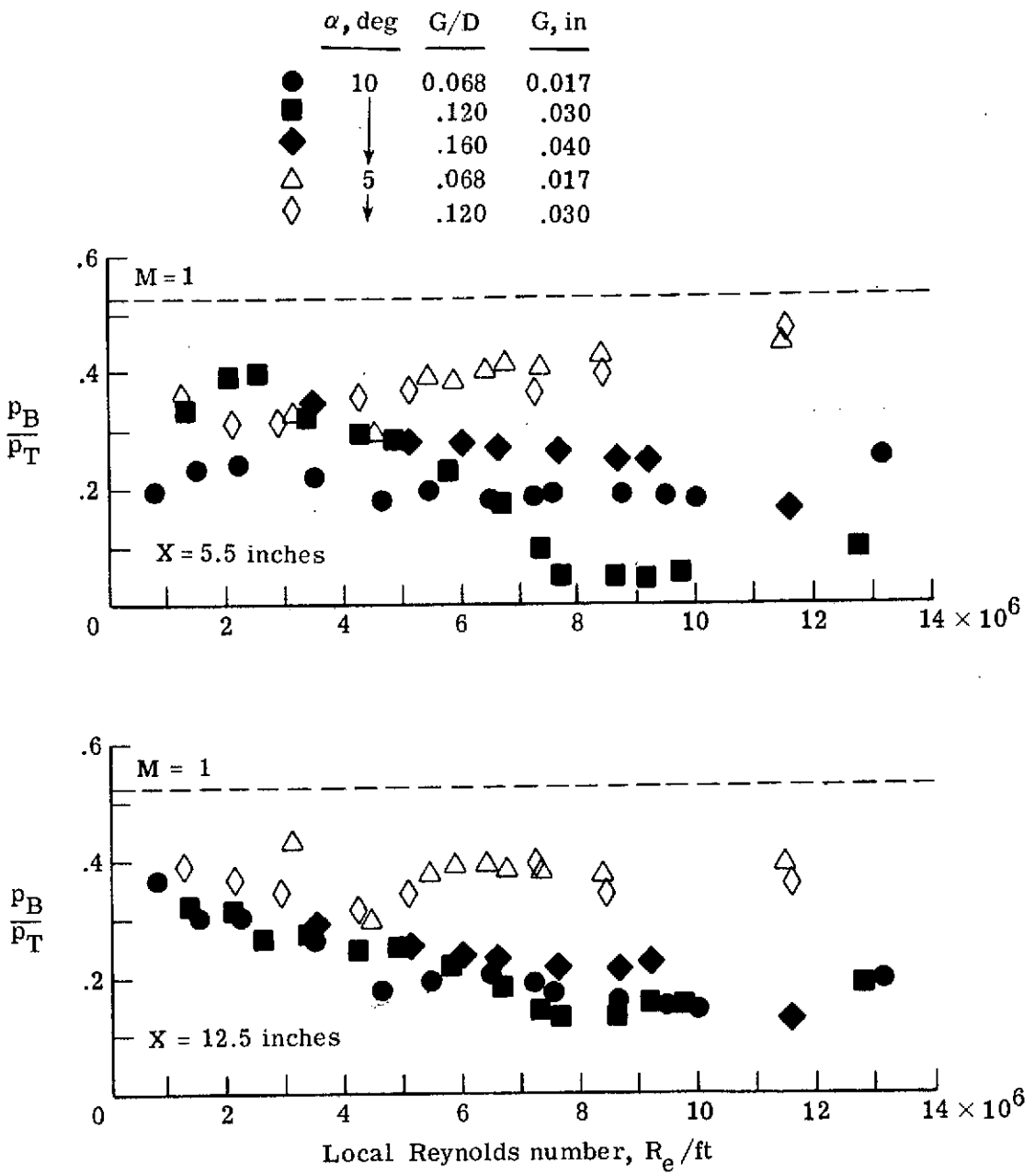

(c) Effect of gap spacing on pressure at bottom of rods.

Figure 7.1.- Concluded.

7.2 Heat Transfer and Transition

The extent of laminar boundary layer flow on the windward side of the circular rods was determined from heat transfer measurements along the stagnation line of the rods. These heat transfer data are compared with laminar and turbulent predictions in Figure 7.2.(a) for Mach 6 at $\alpha = 10^0$ and G/D = 0.16, and with laminar predictions for G/D = 0.12, and 0.068 in Figures 7.2.(b) and (c), respectively. Values of Stanton number for the laminar flow predictions [20] in Figure 7.2 were calculated for values of Re/ft $\geq 6.1 \times 10^6$. However, predicted laminar values of St shown for Re/ft $< 6.1 \times 10^6$ were obtained by the assumption that St varies inversely proportional to the square root of the unit Reynolds number. A discussion of the validity of the boundary layer solutions at low Reynolds number and G/D has been given [17, 20].

No variation of St along the stagnation line is expected from theory [20, 21] when the boundary layer is laminar or turbulent over the entire model. For example, at G/D = 0.16 and the lowest Reynolds numbers of Re/ft $< 8.01 \times 10^6$ (Figure 7.2), the laminar theory predicts the correct level of the data, which were nearly constant along the stagnation line and therefore similar to that along an infinite-swept cylinder for the entire rod length. However, at the higher Reynolds numbers ($8.01 \times 10^6 \leq$ Re/ft $\leq 12.2 \times 10^6$), the experimental values of St agree with laminar theory only over the forward most portion of the model as transition moves forward with increasing Re/ft. At the beginning of transition the heating rates increase, as expected, to peak values followed by a gradual decrease to the predicted turbulent St levels for G/D = 0.16.

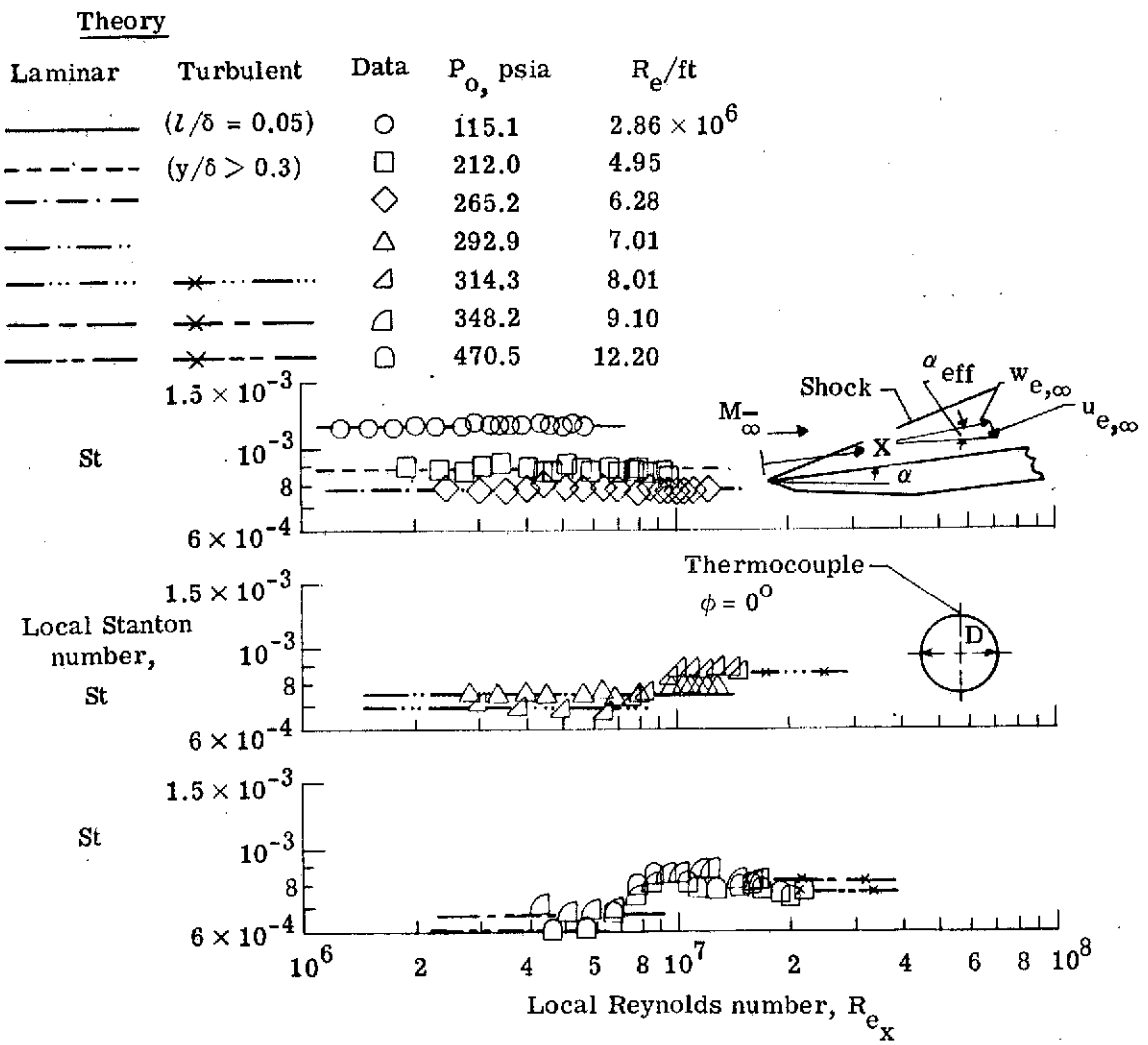

(a) G/D = 0.16

Figure 7.2.- Heat transfer on windward side of rods; $M_\infty = 6$, $\alpha = 10^o$, $T_w = 530^o R$.

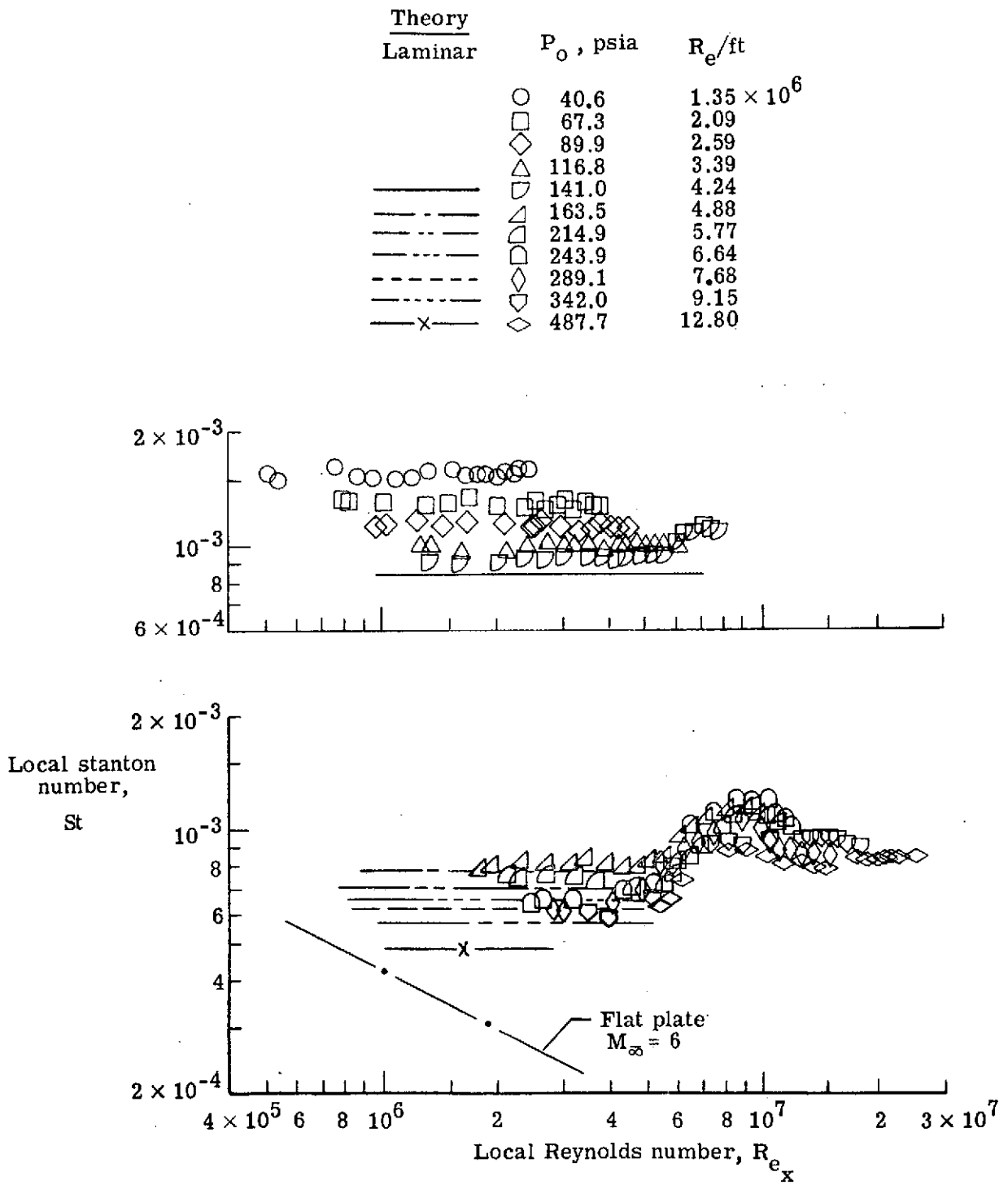

(b) G/D = 0.12

Figure 7.2.- Continued.

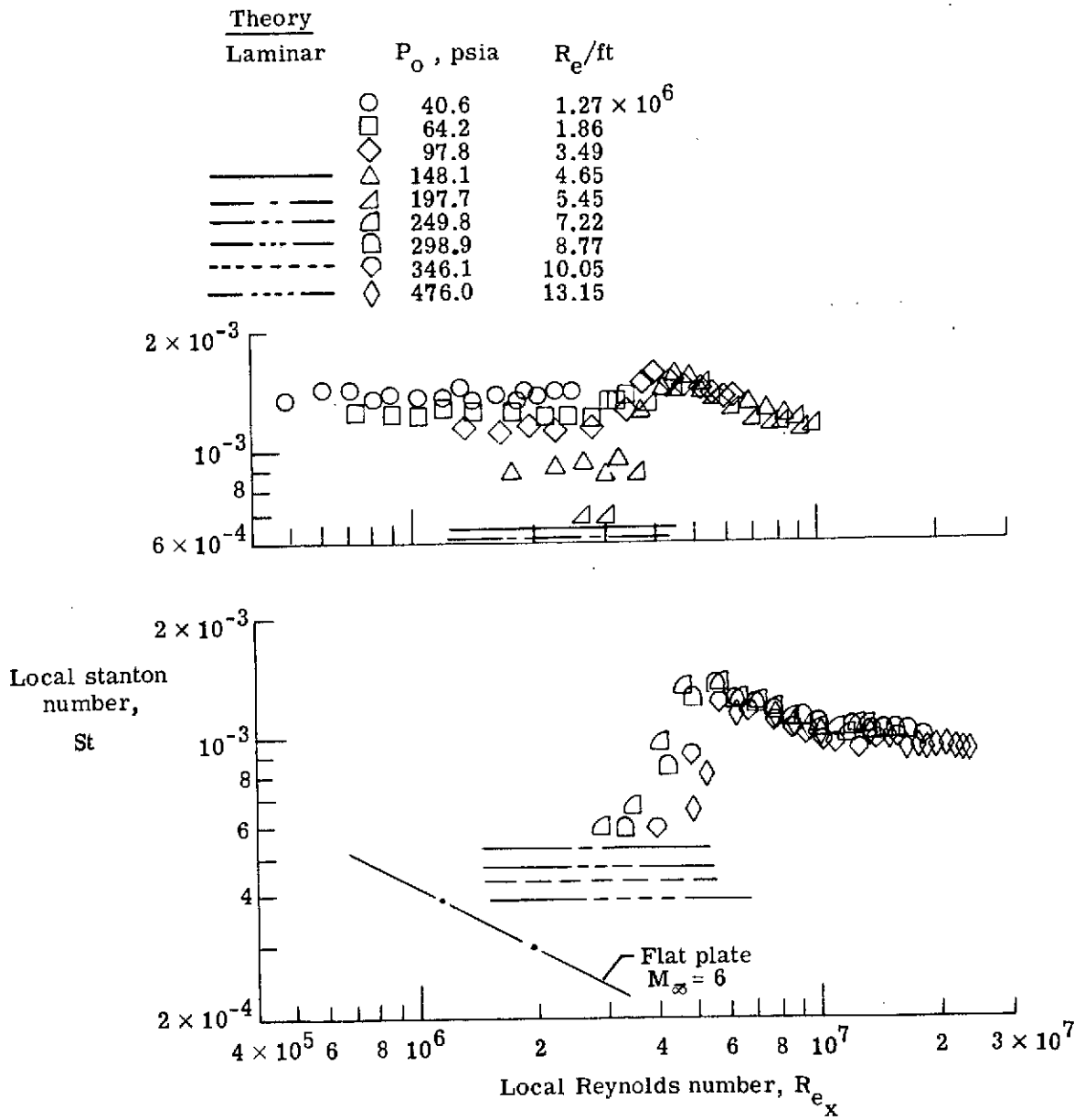

(c) G/D = 0.068

Figure 7.2.- Concluded.

Similar trends in the data and theory comparison for G/D = 0.12 and 0.068 to those for G/D = 0.16 are evident in Figure 7.2. However, the maximum local Reynolds number for the maintenance of laminar flow over the entire model length is seen to decrease with decreasing G/D. Also shown on Figure 7.2 for G/D = 0.12 and 0.068 is the variation of St with Re_x for a conventional flat plate at Mach 6 and $\alpha = 10^o$. Values of the flat plate Stanton number are lower than measured values on the stagnation line of the rods. Calculated values of St for laminar flow (Figs. 7.2.(b) and (c)) are not shown for Re/ft < 4.24×10^6 since rod boundary layer viscous effects have previously been shown [20] to give invalid solutions for reduced G/D and Reynolds number. Measured values of St for G/D = 0.068 (Fig. 7.2.(c)) are much higher than the laminar predictions over the test Reynolds number range possibly due to the presence of discrete vortices on top of the rods to be discussed later. Thus, from comparison of data and theory shown in Figure 7.2, and in spite of the large effective sweep angle of the circular rods with respect to the local flow ($\beta \simeq 89^o$), the heat transfer distribution along the stagnation line is surprisingly similar to that on swept infinite cylinders for G/D = 0.16 and 0.12.

It might be expected that at $\beta \simeq 89^o$ swept cylinder heating would approach the conventional flat plate value (Figure 7.2). An investigation has been made using isolated swept cylinders for β approaching 90^o and the heating rate measured did approach the flat plate value [22]. For the present tests, the induced cross flow velocity was maintained by suction through the gaps (Figure 7.1) and caused the stagnation line

heating to be larger than on a flat plate. For an isolated swept cylinder without induced cross flow, the cross flow velocity would approach zero as β approaches 90^{o} resulting in a reduction in the heating rate for downstream of the tip or leading edge.

7.3 Comparison of Transition Results

The effect of gap spacing on the location of transition on the sound shield over the range of local unit Reynolds number is shown in Figure 7.3 for $0.068 \leq G/D \leq 0.16$. Transition location was chosen at the beginning of the rise in heating observed in Figure 7.2 for $\alpha = 10^{o}$. Results shown in Figure 7.3 for $\alpha = 5^{o}$ were obtained from similar heating data which are not presented herein. Also shown for comparison is a solid line representing transition results obtained on a conventional sharp flat plate at Mach 6 and $\alpha = 10^{o}$ [23]. The solid symbols extending beyond the end of the rod model (dashed line) represents the existence of laminar flow over the entire model length of two feet.

Laminar flow was maintained over the entire model length for maximum values of $(Re/ft)_t$ given on Figure 7.3 for the various values of G/D tested before transition moves on the rear of the model with increasing Re/ft. At a given local unit Reynolds number the present model has a transition Reynolds number considerably higher than the conventional flat plate [23] for all gap spacings tested. The trends for movement of transition forward on the model with increasing Re/ft for G/D = 0.12 and 0.16 is considerably different than the flat plate trend [23]. However, the variations of X_t with Re/ft for G/D = 0.068 and for both $\alpha = 5^{o}$ and 10^{o}

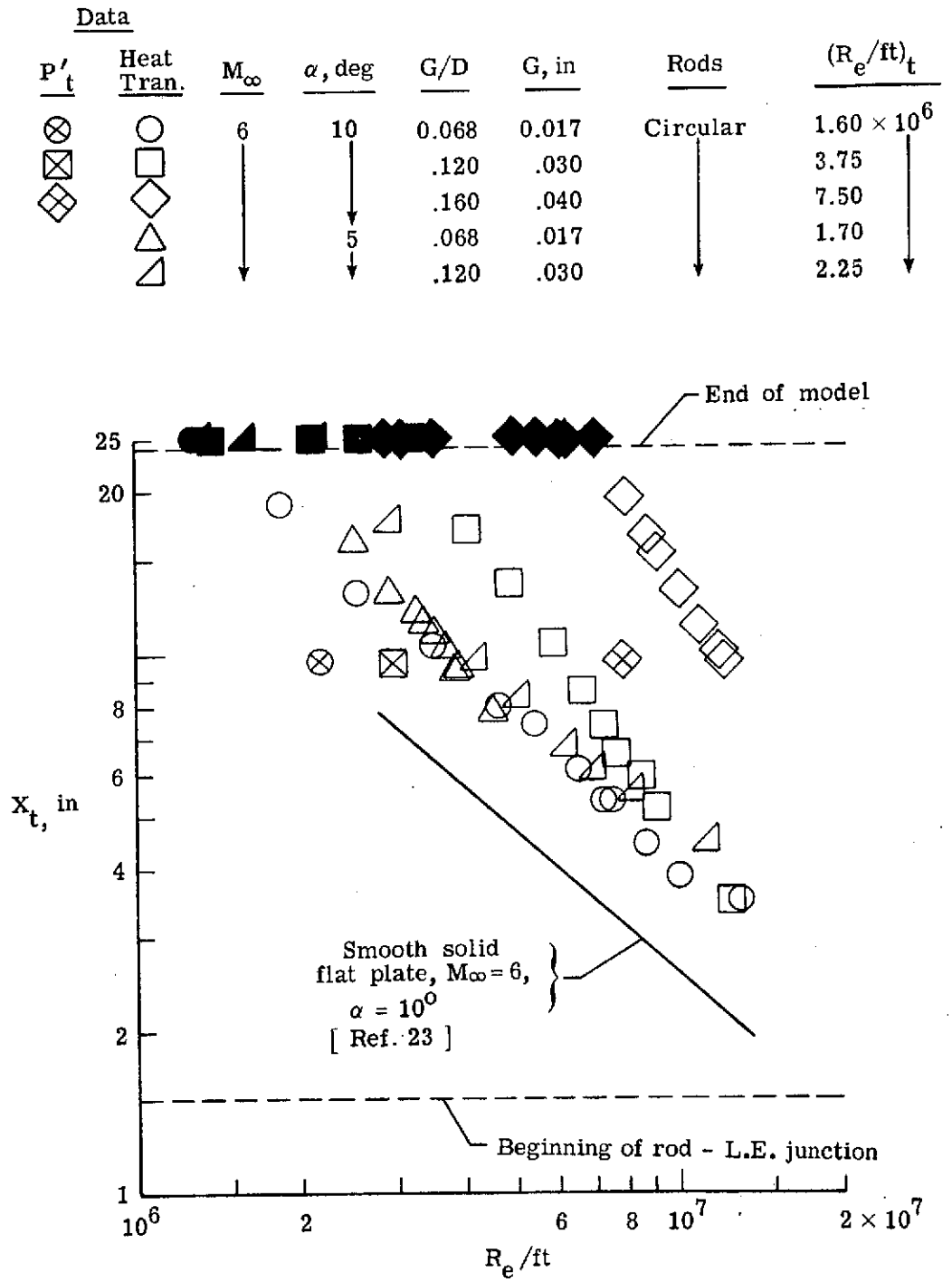

Figure 7.3. - Effect of gap spacing and local unit Reynolds number on transition location.

are nearly the same as that for the flat plate indicating that the movement of transition with Re/ft for these conditions was similar to that of a flat plate. It is concluded that the gap spacing significantly affects the maintenance of laminar flow on the sound shield presumably because of changes in suction mass flow.

Shown in Figure 7.3 are corresponding values of the location for transition on the suction model as measured by the rms pitot probe described earlier [17, 13] for G/D = 0.068, 0.12, and 0.16 and $\alpha = 10^{o}$. The value of x = 9.75-inches corresponds to the upstream acoustic origin on the rods for disturbances that intersect the face of the probe located at x = 15.2-inches and y = 1.125-inches. The probe then responds to transition at this value of x indicated by a sudden increase in p_t' above that measured for laminar flow at lower values of Re/ft. This increase occurred at Re/ft $\simeq 2 \times 10^6$, 3×10^6, and 8×10^6 for values of G/D = 0.068, 0.12, and 0.16, respectively. With the exception of G/D = 0.068, a consistent difference exists between the location of transition at the same Re/ft for the two measuring techniques. The fact that the rms pitot probe indicated that transition occurred on the suction model further forward than indicated by the heat transfer data is probably due to the presence of disturbances or vortices [17] in the gap region of the rod boundary layers.

Maximum length Reynolds numbers for laminar and transitional flow are shown as functions of local unit Reynolds number in Figure 7.3.1 for the circular rod model. Values of $Re_{x,t}$ were chosen at the beginning of

Data	M_∞	α, deg	G/D	$p'/\bar{p}_\infty$ (ref. 6)
Heat trans. data ◇	6	10	0.068	0.014 @ $\frac{R_e}{ft} = 8 \times 10^6$
Heat trans. data △			.120	
Heat trans. data ○			.160	
Begin. of trans., RMS p'_t probe ⊠			.068	0.014 @ $\frac{R_e}{ft} = 8 \times 10^6$
Begin. of trans., RMS p'_t probe ⊠			.120	
Begin. of trans., RMS p'_t probe ⊗			.160	

Note: Open symbols for laminar; solid for onset of transition.

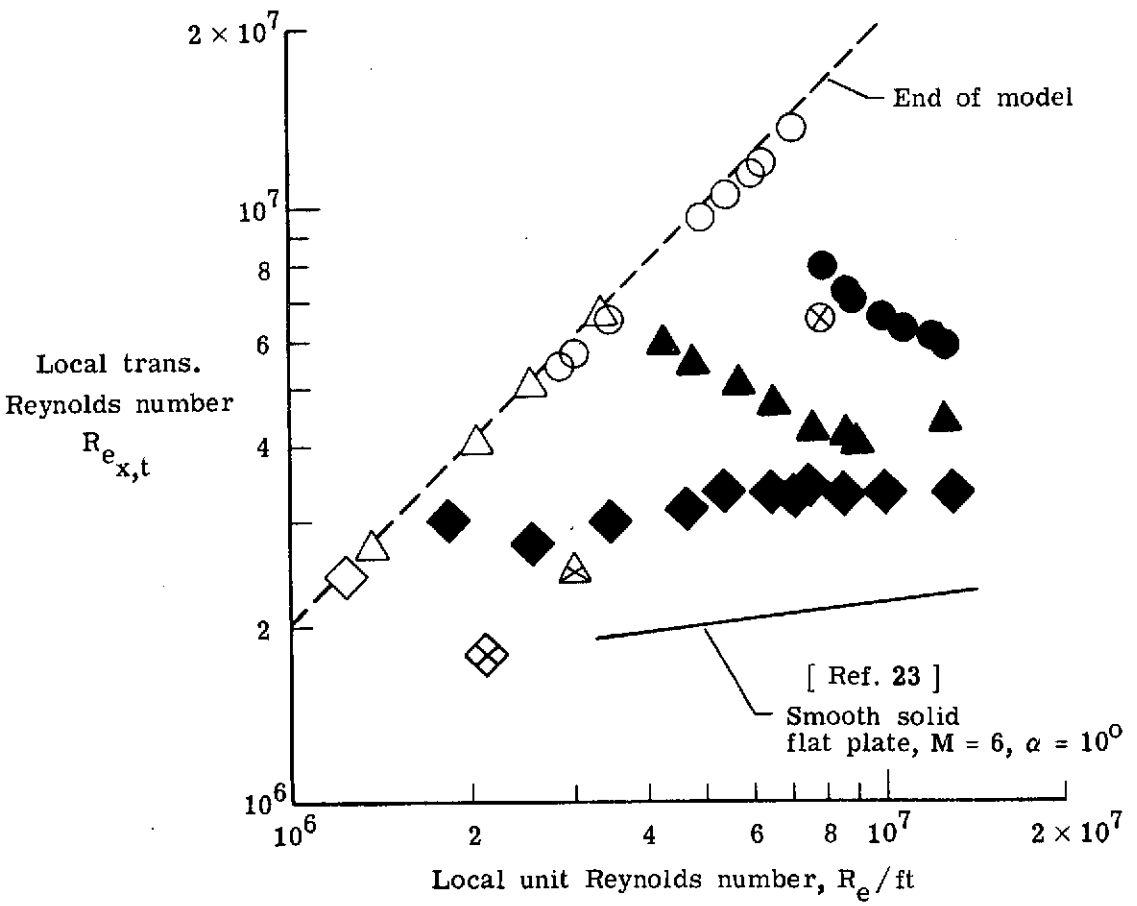

Figure 7.3.1. - Variation of transition Reynolds number with R_e/ft.

transition as indicated by the rise in the heating data from the laminar level as shown earlier in Figure 7.2. Also shown for comparison in Figure 7.3.1 are transition results obtained with the rms pitot probe and a conventional flat plate [23] in the same wind tunnel for $\alpha = 10^{o}$. The present results are shown for $0.068 \leq G/D \leq 0.16$. At a given local unit Reynolds number the rod model has a transition Reynolds number considerably higher than the flat plate [23]. For example, at a local unit Reynolds number of 7×10^{6}, transition for the rod model with $G/D = 0.16$ was just aft of the model base or $Re_{x,t} \simeq 14 \times 10^{6}$. For the flat plate at the same unit Reynolds number, $Re_{x,t} \simeq 2 \times 10^{6}$. For $G/D = 0.068$, the variation of $Re_{x,t}$ with local unit Reynolds number is similar to that for a flat plate [23]. However, this variation is considerably different for $0.12 \leq G/D \leq 0.16$. Apparently, the behavior of transition for $G/D = 0.068$ is similar in trend to that for a flat plate without suction but has higher values of transition Reynolds numbers. Hence, for large values of G/D the present concept satisfies one of the requirements of an effective sound shield, namely; length transition Reynolds numbers that are significantly larger than that expected on a flat plate.

When transition moved onto the model at unit Reynolds numbers of about 3.5×10^{6} and 7.5×10^{6} for $G/D = 0.12$ and 0.16, respectively, there is a rapid decrease in transition Reynolds number with increasing unit Reynolds number. This behavior is not characteristic of a flat plate or wedge. To further investigate this transition behavior, the transition Reynolds numbers based on rod diameter were calculated for the present

tests and compared with results of Bushnell [24]. The calculated values of $Re_{D,t}$ are shown in Figure 7.3.2 for the circular rods at $\alpha = 10^{o}$. An equivalent flat plate transition Reynolds number is also shown for comparison at G/D = 0. This value (Fig. 7.3.2) was obtained from Figure 7.3 by extrapolating the flat plate results of Cary and Morrisette [23] back to the end of the present rod model (x = 24-inches) and then multiplying the corresponding local unit transition Reynolds number by D.

The variation of $Re_{D,t}$ with G/D increases rapidly with increasing gap spacing to a value of $Re_{D,t} \simeq 1.5 \times 10^{5}$ for G/D = 0.16 which agrees well with corresponding values ($1.5 \times 10^{5} \leq Re_{D,t} \leq 2 \times 10^{5}$) on isolated swept cylinders reported by Bushnell [24] where transition was dominated by tip or root disturbances. Also shown on Figure 7.3.2 are calculated values [20] indicating the effect of gap spacing on merging of the boundary layers on adjacent rods at the minimum gap. Merging of the boundary layers occurs for values to the left of the predictions [20]. Valid boundary layer solutions exist to the right of each curve.

It should be noted that the value of $Re_{D,t} \simeq 2 \times 10^{6}$ is for swept cylinders with a pressure distribution and velocity gradient corresponding to isolated cylinder flows [24]. For the present suction model, the pressure distribution [17] and velocity gradient are quite different from that for isolated cylinders. Therefore, it is possible that $Re_{D,t}$ will continue to increase when G/D is increased above 0.16 and the possible effects of leading edge or root disturbances [24] may not dominate transition on this model [25]. In any case, it is concluded that the

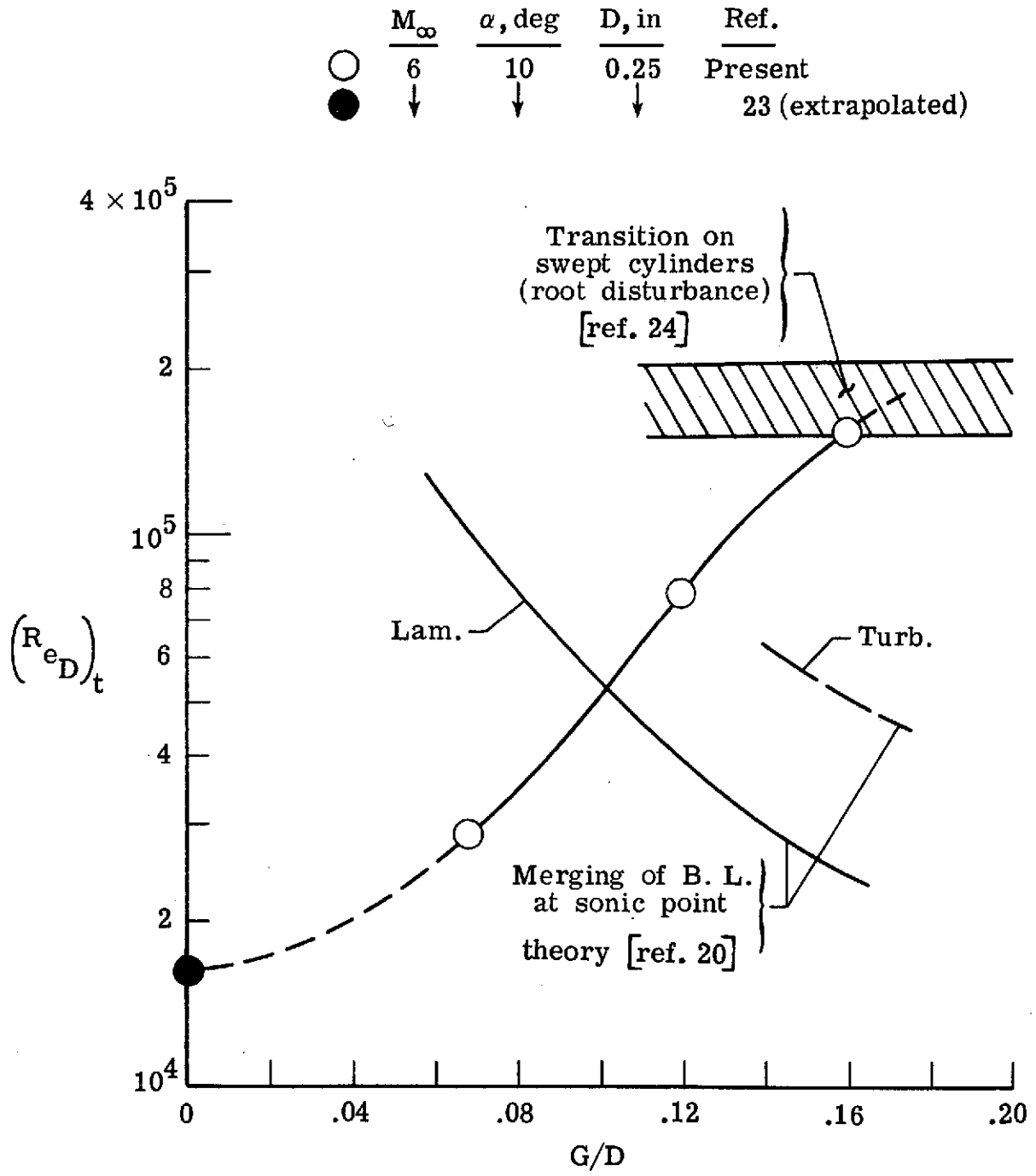

Figure 7.3.2. - Effect of gap spacing on transition Reynolds number based on rod diameter.

boundary layer behavior on the stagnation line of the rods is similar to that on swept cylinders based on experimental heat transfer results. Hence, transition on the circular rods for all gap spacings should be a function of Re_D only and independent of rod length. For example, a 4-foot long sound shield utilizing the present concept with 0.25-inch diameter rods and G/D = 0.16 would be expected to provide a length Reynolds number of 28×10^6 with laminar flow along the entire length based on $(Re/ft)_t = 7 \times 10^6$. Presumably, if leading edge disturbances are important here and if they can be eliminated by improving the fairing at the leading edge (Figure 2.1.1) or by eliminating the effects of the fairing, transition Reynolds number based on rod diameter could be greatly increased [26, 27].

7.4 Visual Observations

Schlieren Photographs. - Representative schlieren photographs of the sound shield are shown in Figure 7.4 for G/D = 0.16 for $Re/ft = 9 \times 10^6$ and Figures 7.4.1 (a), (b), and (c) for G/D = 0.12 and 0.068 for a range of unit Reynolds number. Figure 7.4.1(c) is enlarged photographs of the flow field over the rear of the model ($8 \leq x \leq 10$-inches) for G/D = 0.068. The entire model could not be photographed during a single run and therefore the forward region ($0 \leq x \leq 7$-inches) of the model is shown separate from the rearward portion ($8 \leq x \leq 24$-inches) in Figure 7.4 for G/D = 0.16 at $\alpha = 10^o$. Only the rearward portion of the model ($8 \leq x \leq 24$-inches) is shown in the other figures.

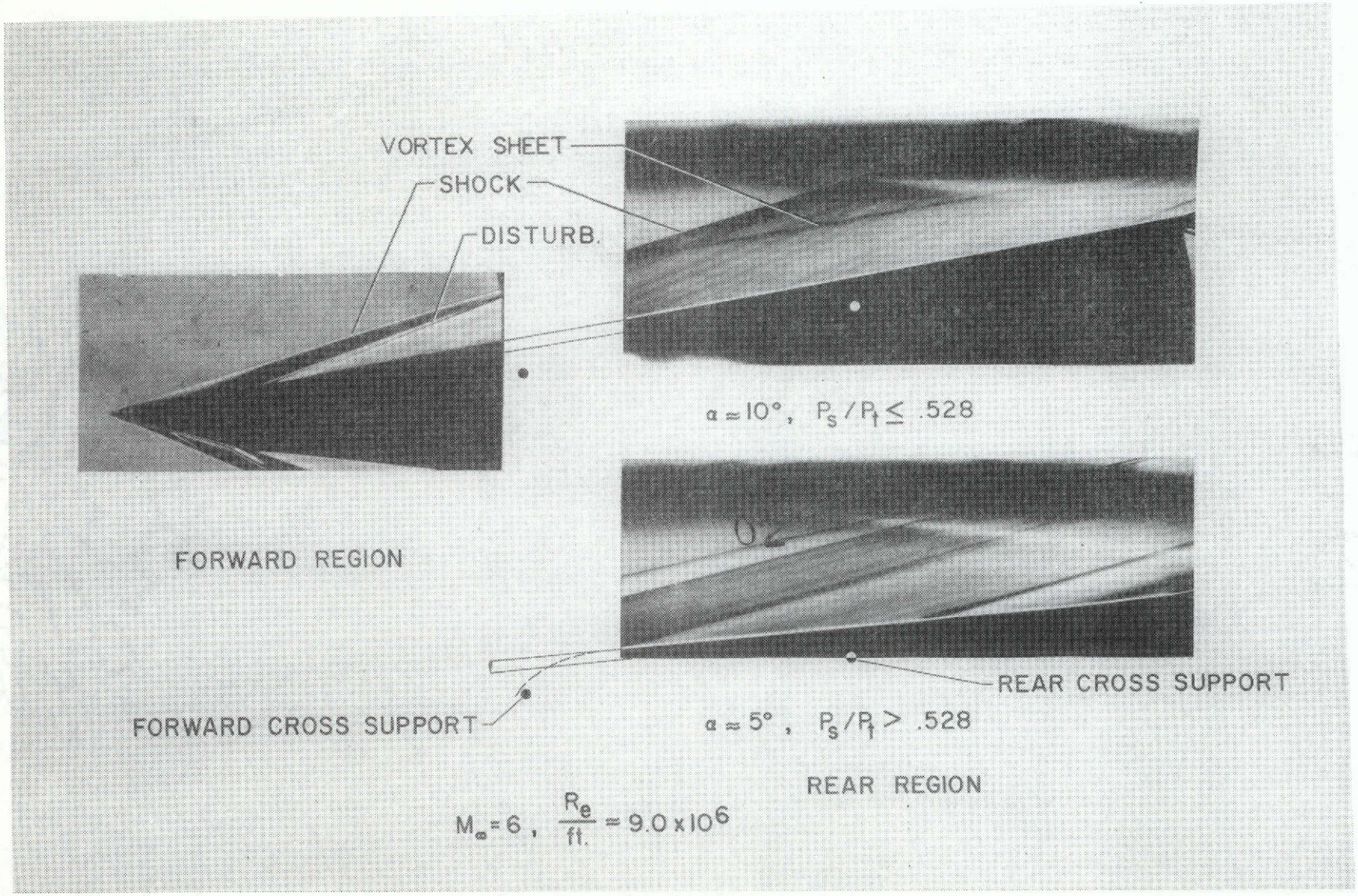

Figure 7.4 Schlieren photographs of circular rod model, G/D = 0.16.

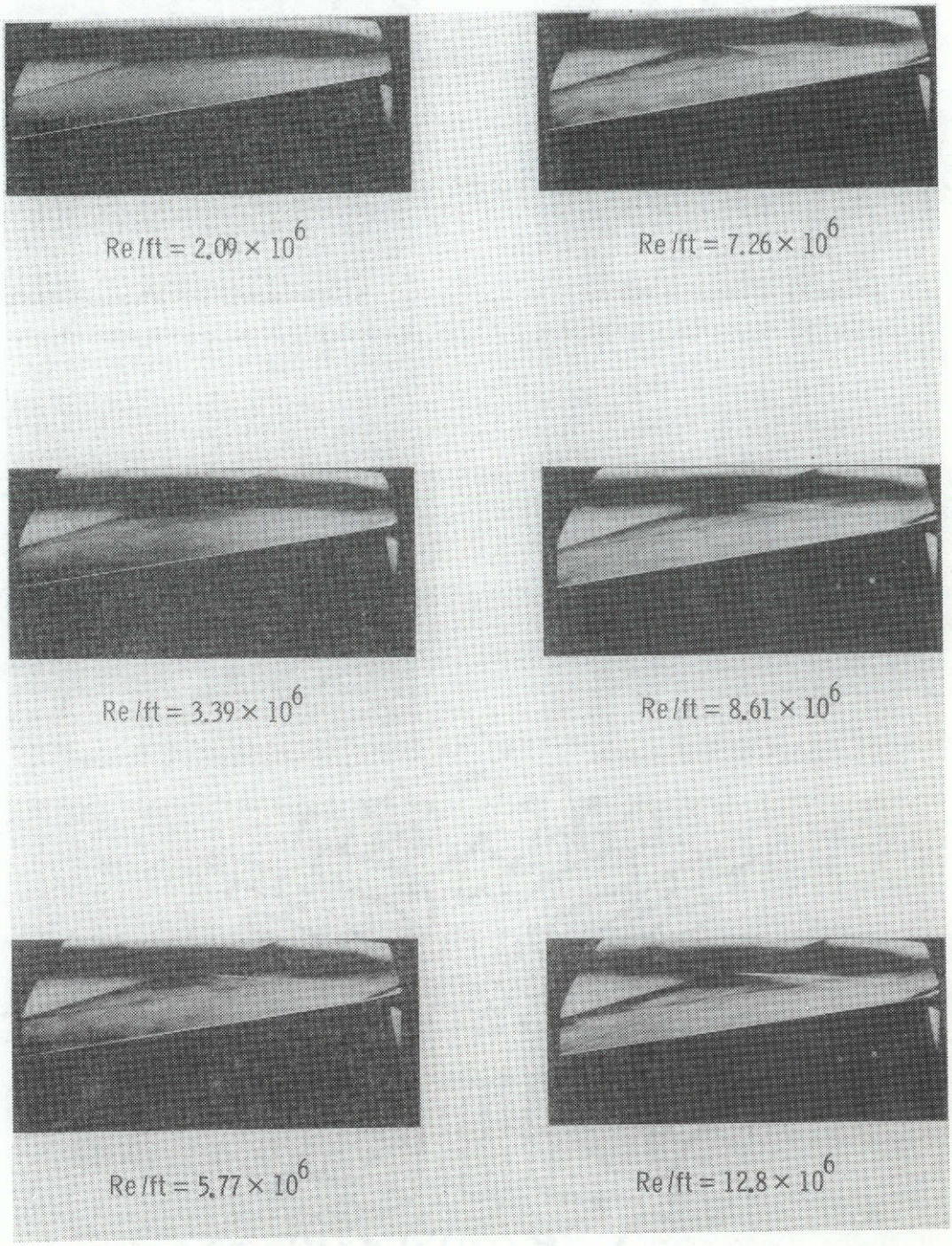

(a) M_∞ = 6, α = 10°, and G/D = 0.12.

Figure 7.4.1.- Schlieren photographs of flow field over rear of flat plate sound shield model with circular rods.

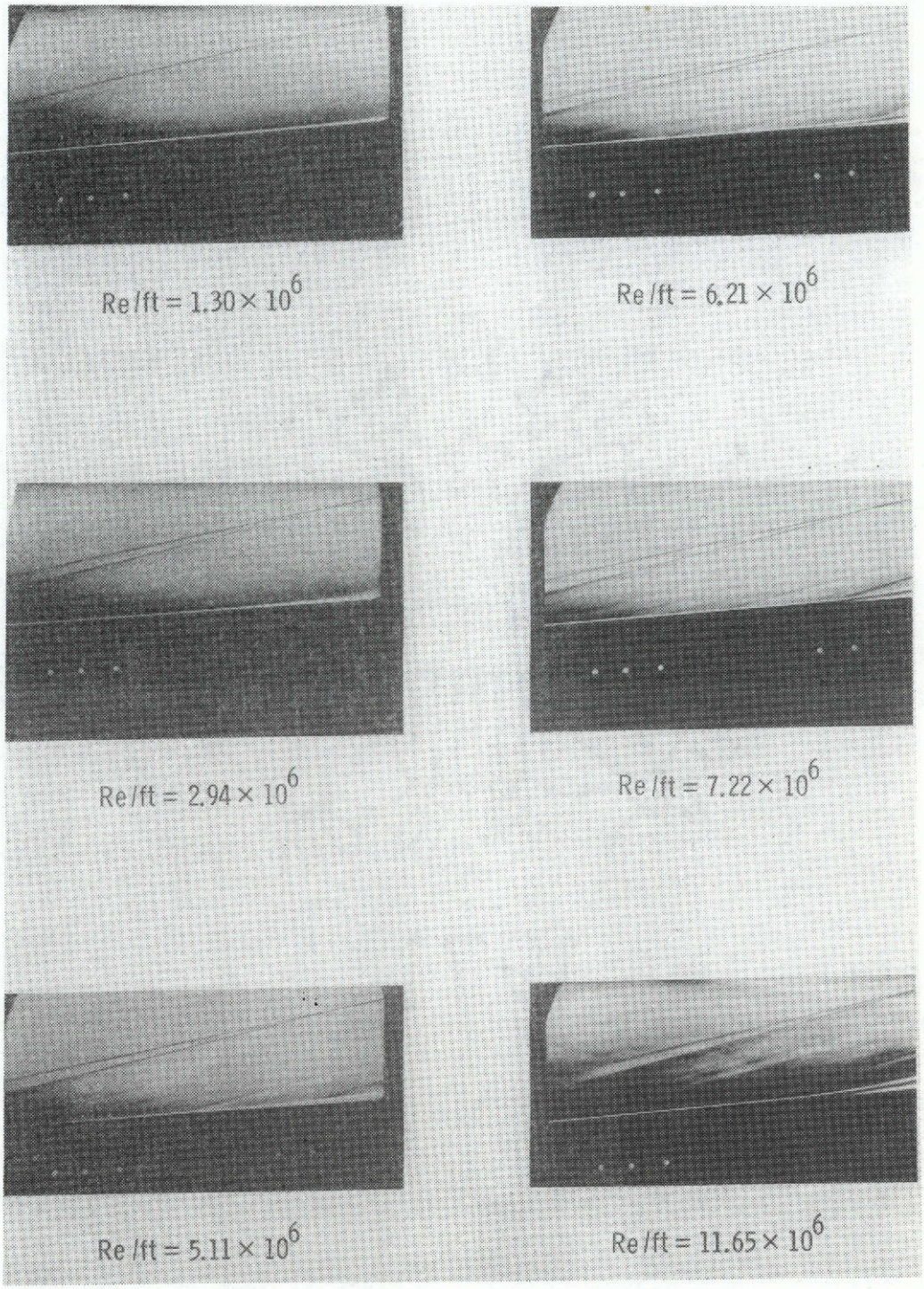

(b) M_∞ = 6, α = 5°, and G/D = 0.12.

Figure 7.4.1 - Continued.

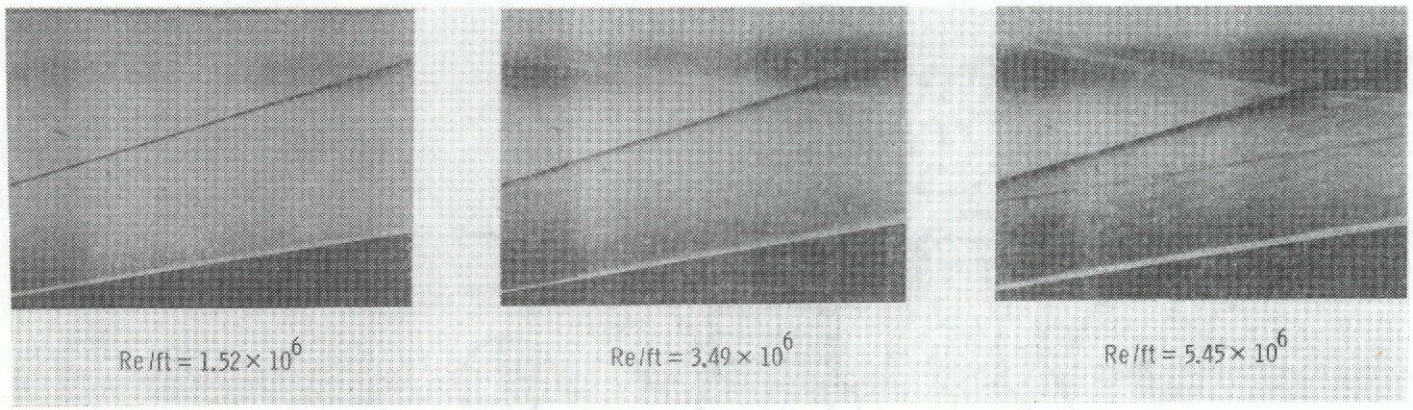

(c) M_∞ = 6, α = 10°, and G/D = 0.068

Figure 7.4.1.- Concluded.

A disturbance (below bow shock) originating in the forward region of the rod model (Fig. 7.4) for G/D = 0.16 and $\alpha = 10^{o}$ was caused by the flat plate leading edge-to-rod fairing (Fig. 2.1). The photographs in Figure 7.4 indicate that this disturbance intersected the bow shock causing a vortex sheet to occur (see rear view). A similar disturbance was present for all values of G/D at $\alpha = 10^{o}$.

A wave pattern in the model flow field (Figs. 7.4 and 7.4.1) downstream of the leading edge region was observed for all tests at Mach 6. The waves are parallel with the local Mach angle in the model flow field. Analysis of the rod gap spacing tolerances and comparison with the test results revealed that the somewhat irregular wave patterns seen in Figures 7.4, 7.4.1.(a), and 7.4.1.(b) were probably caused by longitudinal variations in the gap spacings which were present during tests. Measurements of the rod gap spacing along the model length indicated that a maximum variation of about $\pm$ 0.0020-inches existed at the gaps at random location on the model.

The obviously intense waves also observed in the flow field for $\alpha = 5^{o}$ (Figs. 7.4 and 7.4.1.(b)) are due to the lateral rod support members that induce strong disturbances. The local Mach number is supersonic at the leeside of the gap region of the rod array and in the vicinity of the 0.125-inch diameter rod cross support. Therefore, a shock is produced on the rod cross support by the gap suction flow and this strong disturbance passes back through the gaps and into the shielded region (see Fig. 7.4 for $\alpha = 5^{o}$). The presence of this type of disturbance for

$\alpha = 5^{o}$, in spite of sufficient Δp to generate sonic cross flow (Fig. 7.1.(b)), could definitely be detrimental to the achievement of flow field uniformity. For $\alpha = 5^{o}$ and G/D = 0.12 (Fig. 7.4.1.(b)) the flow near the rods is observed to separate from the surface at the rear of the model with increasing Re/ft. Transition was also found to move on the model and occur for Re/ft $\simeq 1.7 \times 10^{6}$ for this gap spacing and both $\alpha = 5^{o}$ and 10^{o}.

The waves observed in Figure 7.4.1.(c) for G/D = 0.068 appear to be more evenly spaced than in Figures 7.4, 7.4.1.(a) and (b). Hence, the waves at this gap spacing may be the result of some regular flow phenomena. For example, these nearly regular spaced wave patterns could possibly be caused by longitudinal vortex interaction occurring on the rods since such phenomena have previously been observed using the vapor screen technique [17]. The vortex structure on the rod array may interact in the sonic gap flow region at nearly even intervals in the downstream direction producing the observed wavelets. When the suction mass flow is reduced these vortices may become highly unstable and lift off the rods.

The photographs in Figure 7.4.1.(c) for G/D = 0.068 at $\alpha = 10^{o}$ also indicate an increase in either the boundary layer thickness or a change in the previously described presence of vortex flow over the rods with increasing Re/ft as evidenced by the white region in the photographs (Fig. 7.4.1.(c)) along the rod model surface. The observed "double" flow structure on the rods, for example, at Re/ft = 5.45×10^{6} was measured to be about twice that of the calculated boundary layer thickness from

Reference [20] for G/D = 0.068. The measured thickness of the double flow structure corresponds roughly to the observed height of possible discrete vortices present on the rod array and reported earlier [17] for G/D = 0.16 at $\alpha = 10^{o}$. It may, therefore, be concluded that the vortices affect the flow near the rods more at the small gap settings than at G/D = 0.16

Oil Flow. - Oil flow tests were conducted on the rod model at $M_{\infty} = 6$ and $\alpha = 10^{o}$ for $3 \times 10^{6} \leq Re/ft \leq 10 \times 10^{6}$. The techniques used have been previously reported [23, 28, 29]. Representative photographs of oil-flow patterns obtained for laminar and turbulent flow are shown in Reference [17].

Flow turning angle distributions were measured from oil flow photographs [17] at a station located approximately 12-inches from the leading edge of the model. A comparison of the measured flow turning angle in the chordwise direction on the rods with calculated laminar and turbulent values [20] from the swept cylinder theory [21] is shown in Figure 7.4.2 for $M_{\infty} = 6$ and $\alpha = 10^{o}$. In general, data and theory [21] agreed for both laminar and turbulent flow and indicate higher turning angles than for the inviscid flow. The disagreement between data and theory for $\phi > 50^{o}$ is mainly due to the difficulty in obtaining accurately measured values of turning angle ω in this region. It appears, from the agreement shown in Figure 7.4.2 that local flow conditions on the rods can be accurately calculated using the swept cylinder method [21].

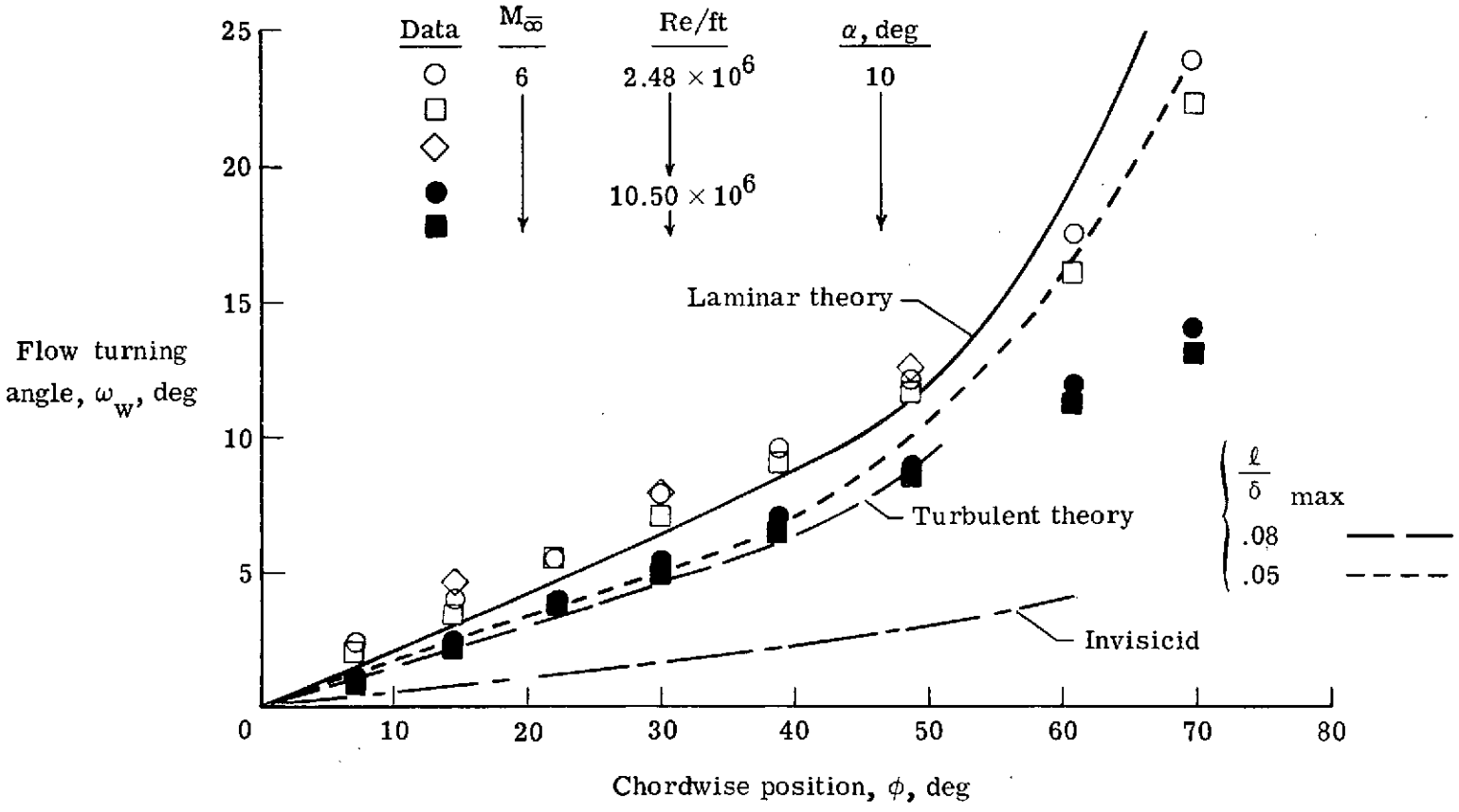

Figure 7.4.2. - Comparison of oil flow turning angle on the rods with theory.

7.5 rms Pressure Fluctuations in Model Flow Field

Pressure fluctuations were measured by P. C. Stainback in the free stream of the wind tunnel and within the partially shielded region (Fig. 1.1) of the rod model flow field. A pitot probe was used to measure the rms pitot pressure fluctuations [13]. The probe was located on the rod model centerline and the probe tip was positioned 1.125-inches above the model at x = 15.2-inches. Tests were conducted for values of G/D = 0.068, 0.12, and 0.16 for $\alpha = 10^{o}$ over a range of local Reynolds numbers (Fig. 7.5).

Measured values of the ratio of rms pressure fluctuations in the model flow field to those in the tunnel free stream at the same unit Reynolds number and with the same probes and transducers are shown in Figure 7.5. The pitot probe responds to noise generated in boundary layers upstream of the probes at acoustic origins [13] of disturbances that intersect the face of the pitot probe pressure transducer. The acoustic origins were determined by extrapolating upstream along local Mach lines from the tip of the pitot probe transducer until the boundary layers on the model or on the tunnel wall were intersected. A corresponding disturbance level measured for a cylindrical shroud with no suction [9] is also shown for comparison in Figure 7.5. Pate and Schueler [9] tested the shroud at Mach 3 and found that about 35 percent attenuation in noise level was achieved at $Re/ft = 1.2 \times 10^{6}$ before transition occurred on the inside walls of the shroud.

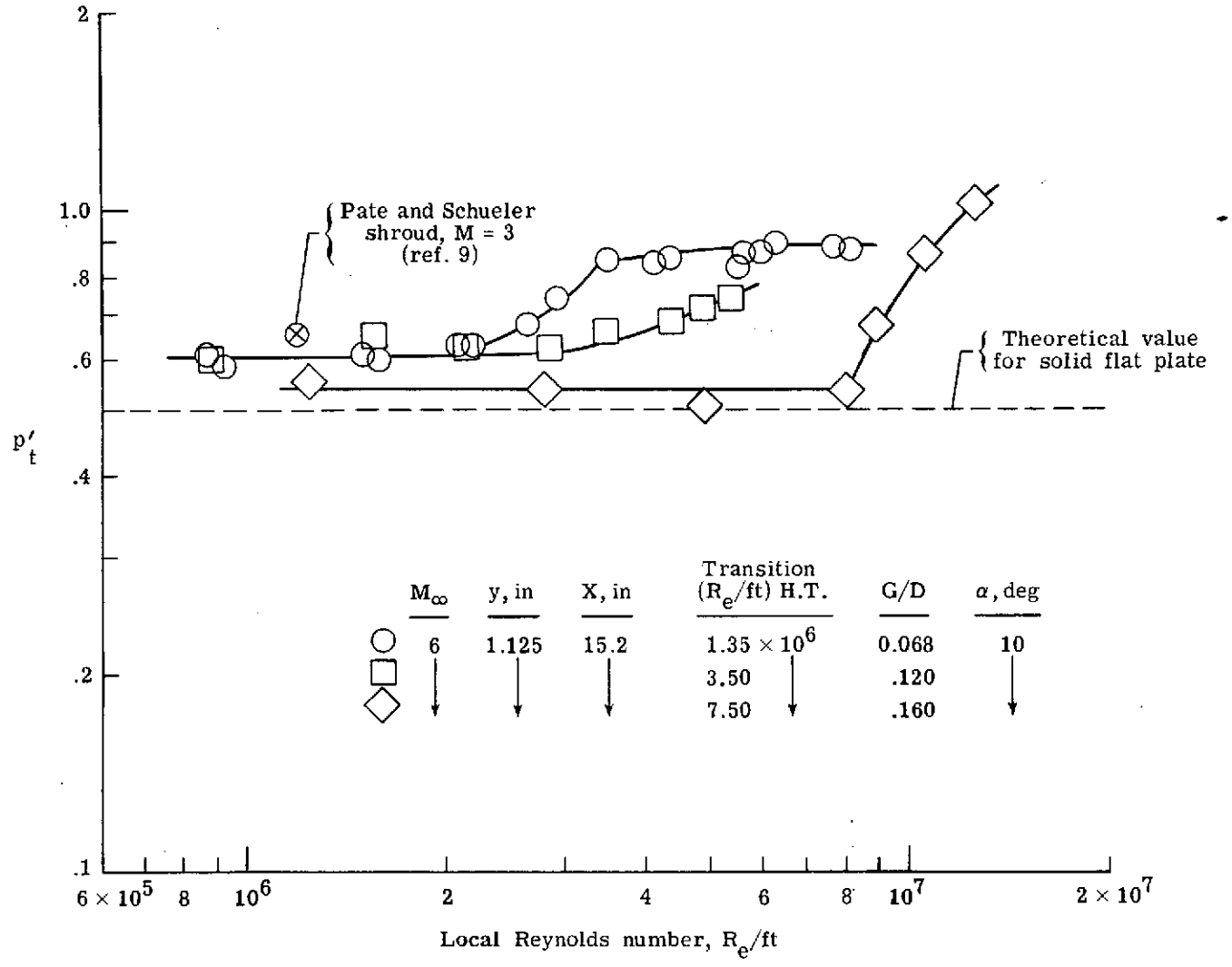

Figure 7.5.- Ratios of RMS pressure fluctuations in the shielded region of model flow field to that in the tunnel free stream.

The important results of the present tests (Fig. 7.5) are that the measured rms pressure fluctuation data obtained with the pitot probe are reduced by as much as 50 percent for the circular rods and G/D = 0.16 until transition occurs at Re/ft $\simeq 8 \times 10^6$. The noise reduction was about 40 percent for G/D = 0.068 and 0.12 before transition occurs at Re/ft $\simeq 2 \times 10^6$ and 3×10^6, respectively. These values of unit Reynolds number for transition obtained from the pressure fluctuations are fairly consistent with the heat transfer data (Figs. 7.2 and 7.3) but the corresponding values of $Re_{x,t}$ differ. This difference may have been expected since the instrumentation used to measure the pressure fluctuations [13] is considerably more sensitive to the presence of disturbances in the flow than that used to measure the heat transfer data. It is possible that disturbances present within the laminar boundary layers on the rods increase in level as the boundary layer becomes unstable before transition occurs [13]. Furthermore, the possible presence of discrete vortices close to the rods as determined by vapor screen studies [17] would also produce disturbances that are related to vortex strength.

The reduction in noise level of about 50 percent is believed to be close to the maximum possible reduction for a planar shield with essentially no reflection of sound from its surface and with little or no sound generation due to boundary layer disturbances on its surface. In support of this statement recall, first, that the rms pitot probe located in the free stream of the tunnel is influenced by noise from the turbulent boundary layers on each wall. However, for a planar shield model that

spans the tunnel, a probe located in the flow field of the model is shielded from noise radiated by the boundary layer on the bottom wall but receives direct radiation from the top wall and one-half of the side walls. The measured noise intensity is thus dependent upon the height of the probe above the rods and view angles with respect to the radiated noise. If the noise generated by each tunnel wall is assumed to be additive in accordance with Laufer's [30] assumption that the mean pressure level in an open tunnel consists of equal contributions from each of the four wind tunnel walls, the noise level attenuation in the flow field of a perfect flat plate shield should be about 50 percent of the free stream value in good agreement with the present results. This agreement further suggests that the boundary layers on the rods did not generate significant noise for G/D = 0.16 up to Re/ft $\simeq 8 \times 10^6$ and the rods effectively prevent reflection of incident noise from the free stream into the model flow field. This apparent prevention of reflected noise into the shielded region is very important for an effective wind tunnel noise shield. However, as the rod gap spacing and suction were reduced the sound attenuation efficiency of the shield was reduced before transition occurred but the attenuation still remains significant. It is therefore concluded that the present rod model, with a laminar boundary layer on the rods and sonic cross flow in the gaps, provided nearly complete shielding (about 90 percent or better of the maximum possible) of the model flow field from noise radiated by the turbulent boundary layer on the nozzle wall. Transmission of noise through the

shield from underneath was prevented by the bottom plate (Fig. 21.) and by sonic flow through the gaps. The application of the present sound shield concept to the design of a quiet tunnel [12, 17] should therefore result in a substantial reduction in the noise level in a test section shielded on all sides [12] when laminar flow is maintained along the entire length of the shield by suction.

7.6 Mean Pitot Pressure Measurements in Model Flow Field

A pitot pressure rake with six equally spaced pitot tubes was used to survey the flow field in a horizontal and verticle plane above the circular rods at $\alpha = 10^{o}$ for G/D = 0.12. The probes were spaced at 0.25-inch intervals across a wedge support. The tubes had an inside diameter of 0.040-inches and outside diameter of 0.060-inches. The mean pitot surveys were conducted in an attempt to evaluate the "flow quality" or uniformity of the mean flow field.

Figure 7.6 (a) shows the ratio of the mean pitot pressure in the model flow field to the calculated stagnation pressure behind the oblique shock as a function of model spanwise location for a range of local unit Reynolds number. The ratios of $p_{t,2}/(p_{t,1})_{cal}$ were obtained from the variation of $p_{t,2}/p_{o}$ with Re/ft shown in Figure 7.6(b) and the calculated value of $p_{t,1}$ behind the oblique shock on the flat plate rod model. The location of the rod gaps for G/D = 0.12 (Fig. 7.6(a)) are indicated on the horizontal axis to show the probe locations with respect to the gaps and rods. The rake was located 1.125-inches above the rods at x = 15.2-inches. The data indicate deviations in pitot pressure and Mach number in

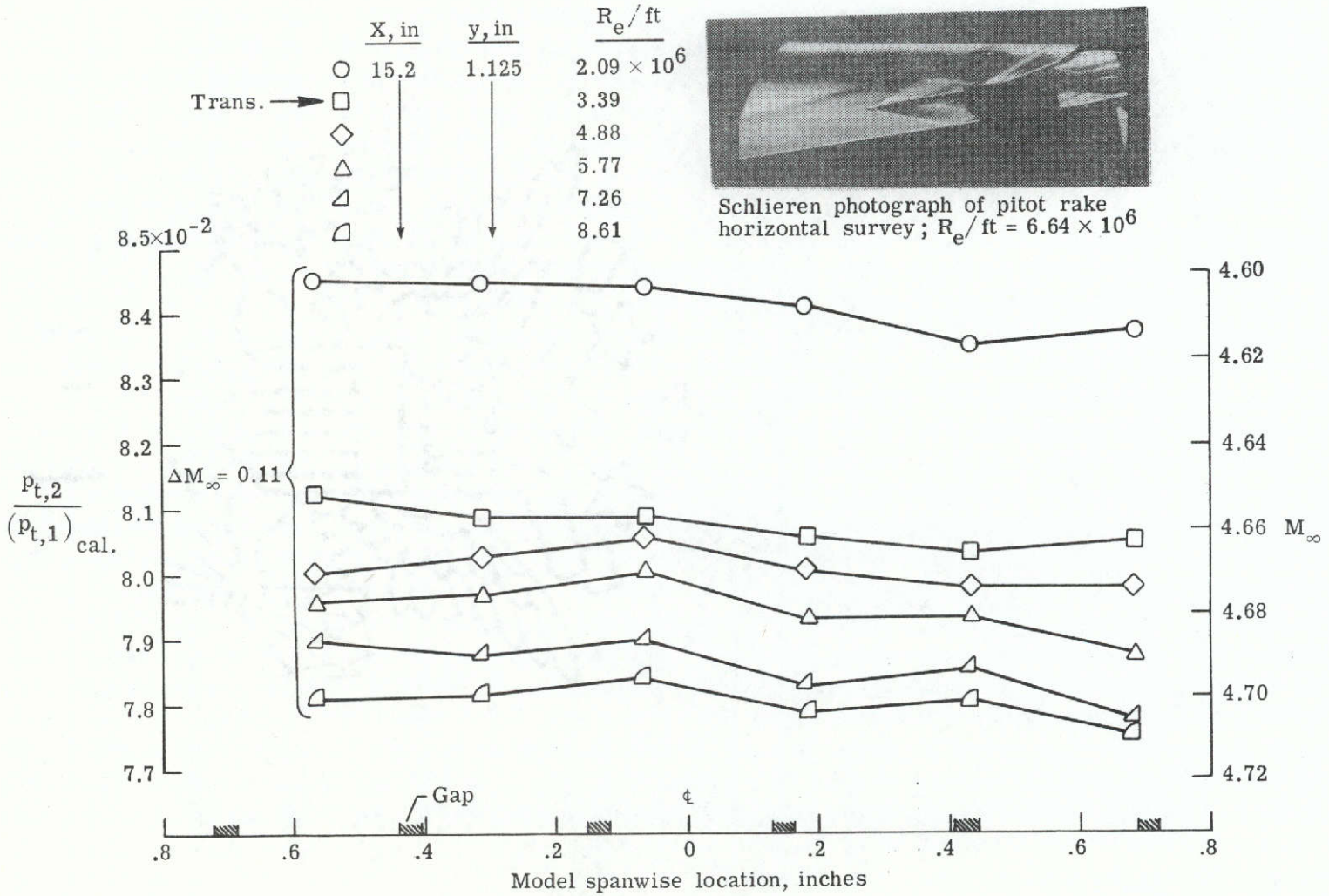

(a) Horizontal survey of model flowfield

Figure 7.6. - Survey of mean pitot pressure in flowfield of rod model, $\alpha = 10^o$, and G/D = 0.12.

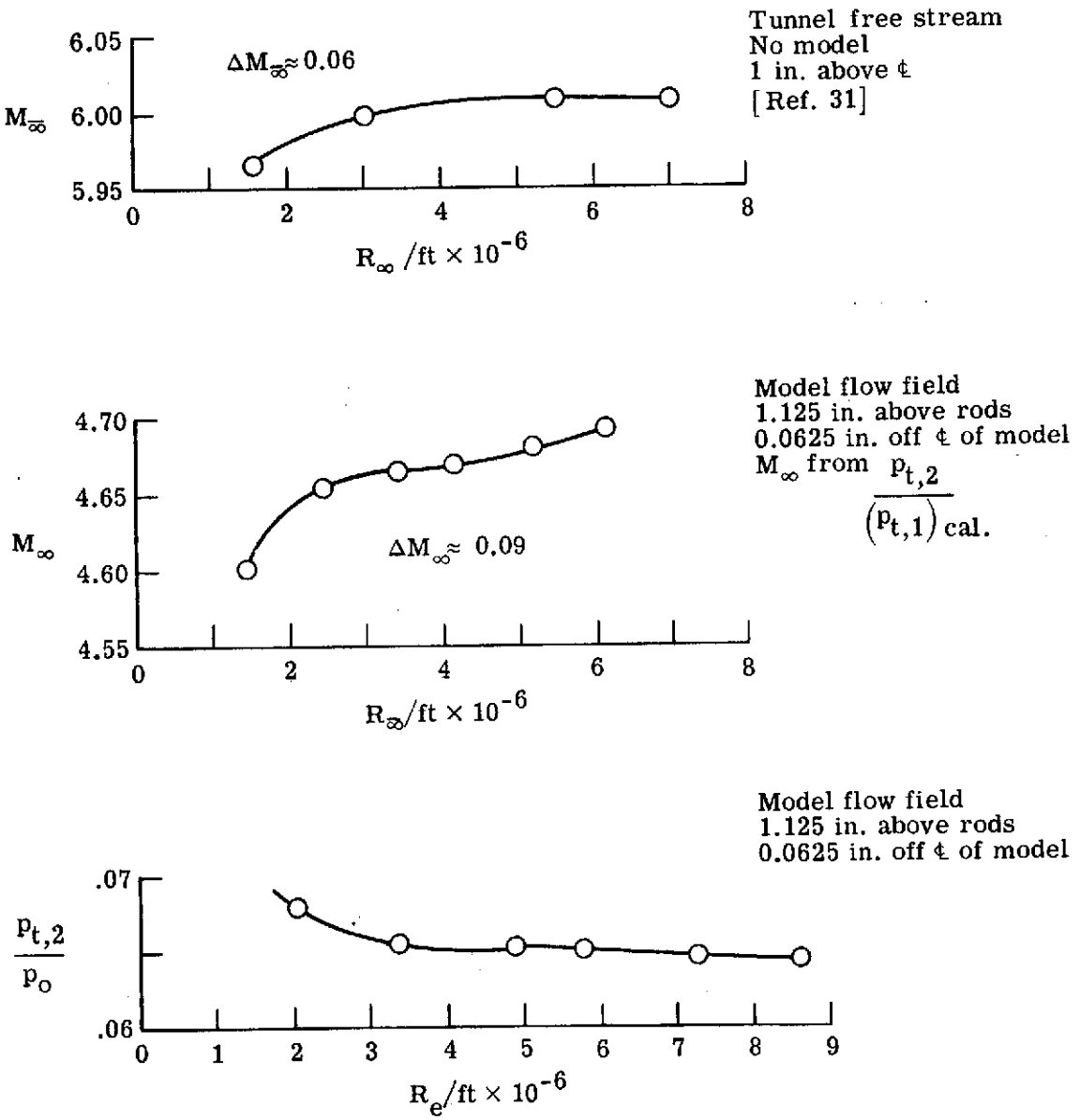

(b) Comparison of model flowfield results with tunnel free stream calibration

Figure 7.6.- Concluded.

the model spanwise direction for all values of Re/ft. The maximum change in Mach number in the spanwise direction is about $\Delta M_\infty = 0.02$ for a given value of Re/ft. The average spanwise pressure level decreases with increasing local unit Reynolds number with a maximum change in Mach number of about $\Delta M_\infty = 0.11$. The quality of the model flow field is believed to be satisfactory at this station above the rods (y = 1.125-inches) even though the pressure distribution is changing in the spanwise direction with increasing Re/ft. Figure 7.6 (b) gives the variation with unit Reynolds number of the model flow field results at a single station of 1.125-inches above the rods and 0.0625-inches off the model centerline. The tunnel free stream calibration [31] at one inch above the tunnel centerline and same longitudinal location but without the model in place is also given in Figure 7.6 (b). The variation with unit Reynolds number of the local Mach number (M_∞), obtained from $p_{t,2}/(p_{t,1})_{cal}$ in the model flow field, is about $\Delta M_\infty = 0.09$ and nearly the same as the corresponding variation of the free stream Mach number ($\Delta M_\infty \simeq 0.06$) in the wind tunnel [31].

Figure 7.6.1 shows pitot pressure profiles in the model flow field normal to the top of the 0.25-inch diameter rod located on the model centerline as a function of distance above the rod. With the exception of the data very near the top of the rod (y = 0.0625), the results indicate that the quality of the flow is good for all Reynolds numbers tested. These results are in agreement with those presented in Figure 7.6 (a) for the spanwise surveys. An increase in level of the data near

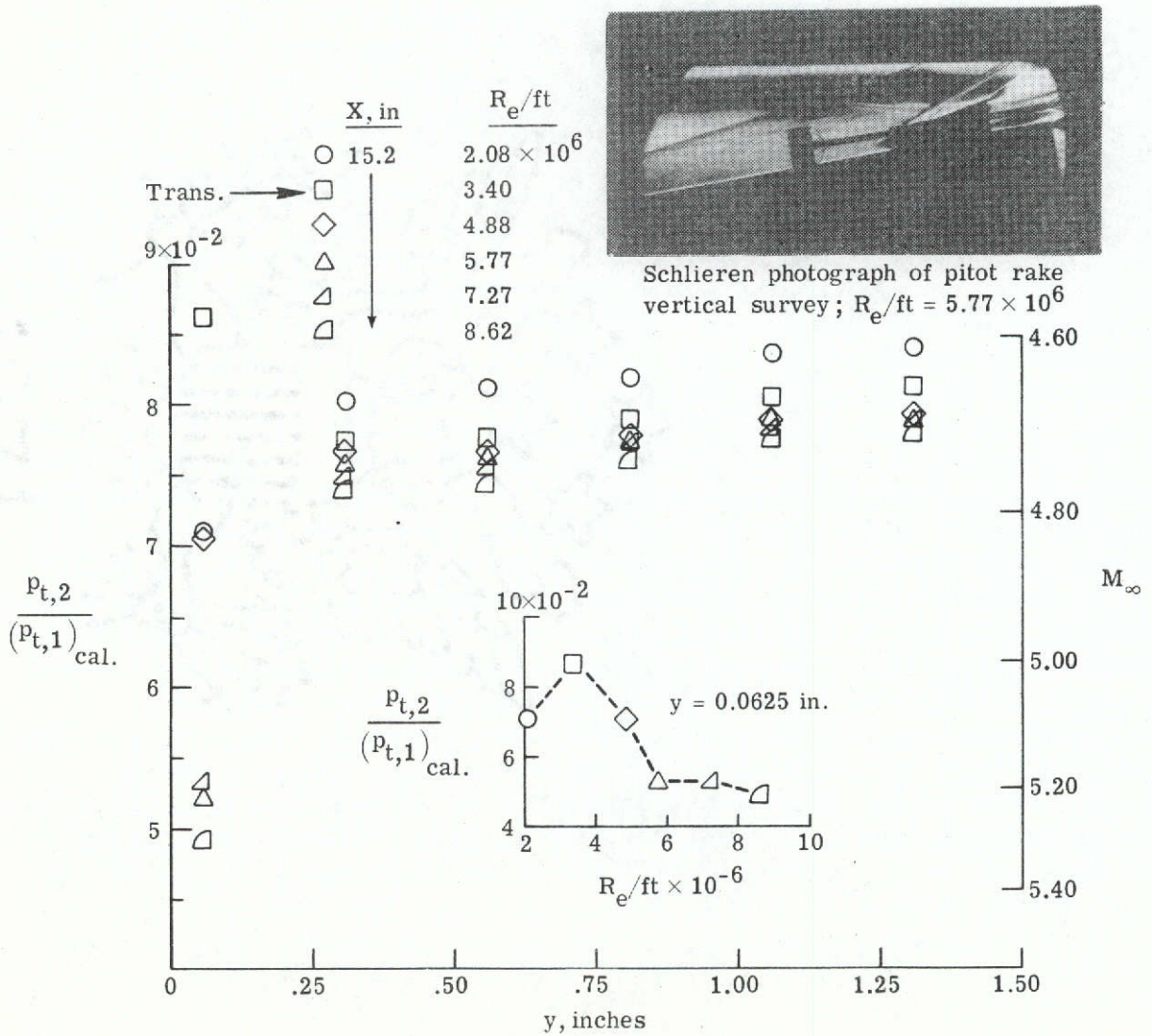

Figure 7.6.1. - Flowfield survey of mean pitot pressure centered over rod on model centerline. $\alpha = 10^o$, G/D = 0.12.

the top of the rod (y = 0.0625) with Re/ft before decreasing again with a further increase in Reynolds number (see insert in Fig. 7.6.1) is believed to be due to the presence of that probe in or near the rod boundary layer. This variation in pressure near the rod with Re/ft is a possible indication of transition of the rod boundary layer and would require further investigation for verification. One other possibility is that this probe located near the top of the rod was in the immediate region of discrete vortices [17] above the rods. The observed variation in pressure may then be a result of changes in vortex strength or movement with increasing Re/ft. This preliminary evaluation of the model flow field for a single gap spacing is not conclusive, however, these limited results indicate that the flow quality in the shielded region is satisfactory for normal distances greater than about one rod diameter above the rod array and over the center portion of the model span.

VIII. APPLICATION OF SOUND SHIELD CONCEPT

8.1 Langley Quiet Tunnel Sound Shield

The sound shield concept considered in this thesis is planar and is intended to test the concepts to be used for an actual sound shield that would enclose the entire test section of a wind tunnel. A cylindrical sound shield constructed of longitudinal rods is currently being tested in the Langley Pilot Quiet Tunnel [32]. The configuration is illustrated in Figure 8.1 and presents some difficult design, construction, and flow field analysis problems. Experience gained from the present flat plate

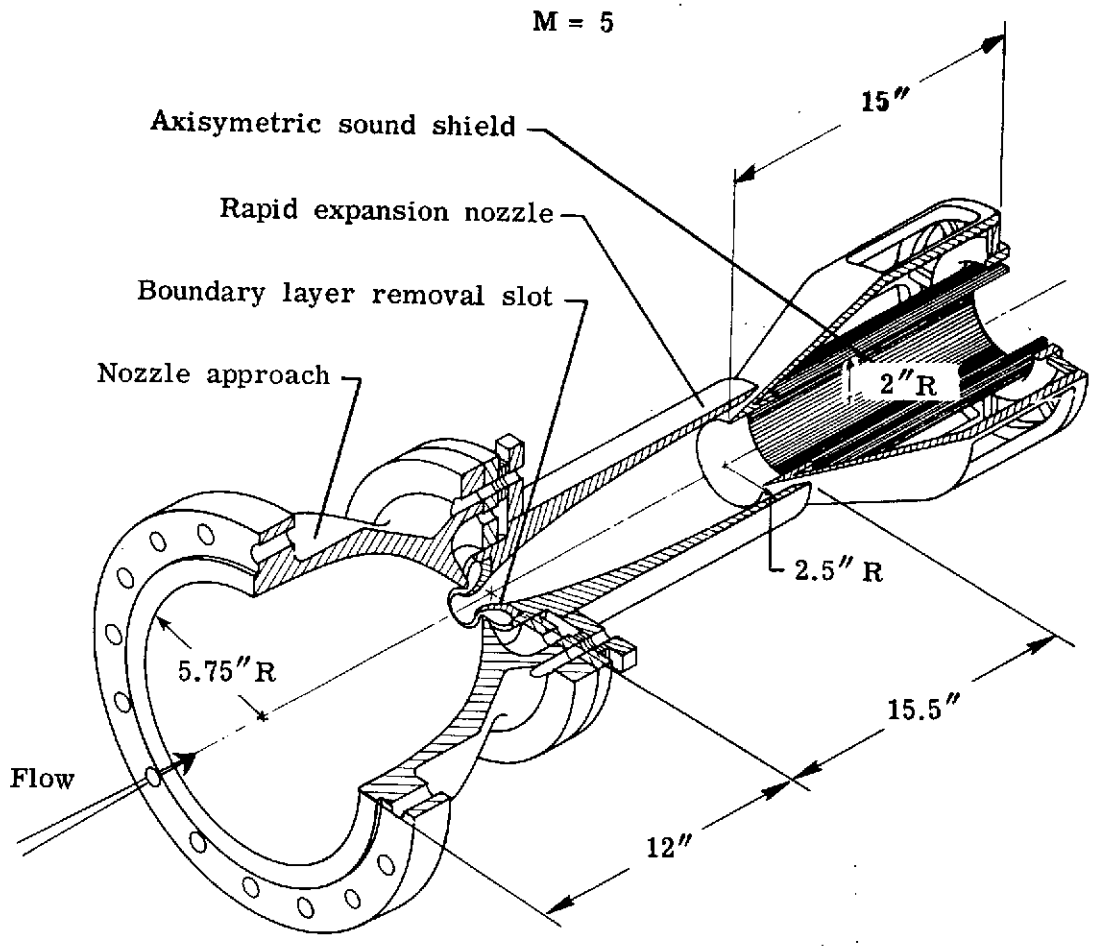

Figure 8.1.- Pilot quiet tunnel and sound shield.

sound shield was used in the development of the axisymmetric sound shield [32]. The entire assembly is mounted within a vacuum chamber. There is an annular scoop transverse to the flow in the subsonic portion of the nozzle to remove the turbulent boundary layer that develops upstream of the slot [33]. Using this design technique [32], a laminar boundary layer is started just upstream of the nozzle throat and transition should be delayed on the nozzle wall provided the slot does not introduce additional disturbances that would also enter the shield flow field.

The axisymmetric sound shield (Fig. 8.1) is mounted at the exit of the slotted nozzle. The rods are aligned with the exit free stream flow and arranged cylindrically to provide complete shielding of the enclosed test region from sound radiation by the boundary layer and free shear layer. The gaps between the rods are adjustable and flow through the rods is exhausted into a vacuum manifold to maintain the pressure on the leeside of the rods equal to or less than (0.528) of free stream static pressure inside the shield. Cross flow normal to the rods is thereby accelerated to sonic velocity at the minimum gap width. The sharp leading edge of the sound shield is just inside the nozzle internal diameter and serves as a scoop to remove the turbulent boundary layer on the nozzle wall. The laminar boundary layer forming on the inside wall of the shield is partially removed through the gaps.

Preliminary tests on the small axisymmetric sound shield (Fig. 8.1) with G/D = 0.068 have been conducted at Mach 5 [32]. The results showed that at the lowest test Reynolds number based on rod diameter of 5.2×10^4,

the shield reduced the test section noise by about 60 percent (or 8 dB attenuation) but very little attenuation was measured for higher Reynolds numbers up to 1.9×10^5. The results were below expectations based on results herein and were attributed to insufficient suction at the gaps to prevent feedback of vacuum manifold noise into the shielded region and the prevention of transition of the rod boundary layers to turbulent flow at the higher test Reynolds numbers. Increased gap spacing and vacuum mass flow capability will be required to obtain the large sound attenuation and transition Reynolds numbers that would be expected based on the present planar sound shield results.

CONCLUDING REMARKS

To obtain low levels of stream disturbances at high test Reynolds numbers in supersonic wind tunnels, noise radiation shields will be required. Therefore, an experimental and theoretical investigation has been conducted on a conceptual noise shield model. The model consisted of circular rods aligned with the flow with adjustable gaps between the rods for boundary layer suction. Results are reported at Mach number 6 for a wide range of local Reynolds numbers and for gap-to-rod diameter ratios of 0.068, 0.12, and 0.16.

The effective sweep angle of the rods with respect to the local flow was very large ($\beta \simeq 89^\circ$), nevertheless, the boundary layer behavior on the rods was surprisingly well represented by swept cylinder theory. With boundary layer removal by induced suction through the rod gaps,

laminar flow can be maintained on the rod shield model up to a local Reynolds number per foot of 7.5×10^6 for a gap-to-rod diameter ratio of G/D = 0.16. The maximum local Reynolds number where transition occurred on the planar shield model for this gap spacing was about 15×10^6, which is about 7.5 times higher than that for a conventional flat plate at the same local unit Reynolds number and in the same wind tunnel. Less favorable results were obtained with decreasing gap-to-diameter ratio. Transition Reynolds number was found to decrease by about a factor of two with reduced gap spacings of G/D = 0.12 and 0.068 and the corresponding reduced suction mass flow. However, the model still provided a significant increase in transition Reynolds numbers above that for a flat plate without suction. Transition moved rapidly forward on the suction model with further increases in local Reynolds number, with a trend unlike that for a flat plate for the two largest gap spacings. The forward movement of transition on the model for G/D = 0.068 is similar in trend to that for a flat plate. Hence for G/D = 0.068, the boundary layer behavior is similar to that for a flat plate.

A comparison of the present transition results for the circular rods with correlations on swept cylinders indicated that for G/D = 0.16, transition may be dominated by leading edge or "root" disturbances. Since the general properties and transition behavior of the boundary layers on the rods are similar to those on swept cylinders, transition would be essentially independent of rod length and primarily a function of Reynolds number based on rod diameter for a given gap spacing and leading edge configuration.

Sound levels measured in the semi-shielded region of the model showed that nearly 90 percent (20 dB attenuation) of the maximum theoretical possible noise attenuation was achieved with sonic cross flow suction at the gaps and laminar boundary layer on the rods for G/D = 0.16. However, reduced gap spacing and suction caused both a reduction in transition Reynolds number and in the sound attenuation that could be achieved. These results are in agreement with the transition results obtained from measured heat transfer data.

Evidence of wave patterns present in the model flow field and possible discrete vortices very near the rod array surfaces was found. The somewhat irregular spaced wave patterns observed for the two largest gap spacings and 10^{o} angle of attack were attributed to measured errors in gap spacing. The more regular spaced wave patterns observed for G/D = 0.068 were possibly due to the interaction of adjacent vortices at the sonic gap flow region between the rods. A preliminary evaluation of the model flow field for a single gap spacing based on limited results indicate that the flow quality in the model shielded region is satisfactory for normal distances greater than about one rod diameter above the rod array and over the center portion of the model.

It is concluded that a cylindrical shroud utilizing the slotted wall concept and boundary layer suction can provide significant reduction of disturbance levels in supersonic wind tunnels at high Reynolds number. However, gap spacings on the order of G/D = 0.16 may be required to achieve desired results.

REFERENCES

1. Morkovin, M. V.: "Critical Evaluation of Transition From Laminar to Turbulent Shear Layers With Emphasis on Hypersonically Traveling Bodies." Air Force Flight Dynamics Laboratory, AFFDL-TR-68-149, 1969.

2. Laufer, J.: "Stability of the Laminar Boundary Layer." I.U.T.A.M. Symposium on Boundary Layer Research, Freiburg, p. 139, Springer-Verlag, Berlin, 1958.

3. Laufer, J.: "Factors Affecting Transition Reynolds Numbers on Models in Supersonic Wind Tunnels." Journal of the Aeronautical Sciences, Vol. 21, July 1954, pp. 497-498.

4. Mack, L. M.: "On the Application of Linear Stability Theory to the Problems of Supersonic Boundary Layer Transition." AIAA Paper No. 74-134, presented at 12th Aerospace Sciences Meeting, January 30-February 1, 1974.

5. Wagner, R. D.; Maddalon, D. V.; and Weinstein, L. M.: "Influence of Measured Free Stream Disturbances on Hypersonic Boundary Layer Transition." AIAA Journal, Vol. 8, No. 9, September 1970, pp. 1664-1670.

6. Stainback, P. C.; Fischer, M. C.; and Wagner, R. D.: "Effects of Wind Tunnel Disturbances on Hypersonic Boundary-Layer Transition," Parts I and II. AIAA Paper No. 72-181, January 1972.

7. Kendall, J. M.: "Wind Tunnel Experiments Relating to Supersonic and Hypersonic Boundary Layer Transition." AIAA Paper 74-133. AIAA 12th Aerospace Sciences Meeting, January 30-February 1, 1974.

8. Stainback, P. C.; Wagner, R. D.; Owen, F. K.; and Horstman, C. C.: "Experimental Studies of Hypersonic Boundary Layer Transition and Effects of Wind Tunnel Disturbances." NASA TN D-7453, March 1974.

9. Pate, S. R.; and Schueler, C. J.: "Radiated Aerodynamic Noise Effects on Boundary Layer Transition in Supersonic and Hypersonic Wind Tunnels." AIAA Journal, Vol. 7, No. 3, March 1969.

10. Fischer, M. C.; and Ash, R. L.: "A General Review of Concepts for Reducing Skin Friction, Including Recommendations for Future Studies." NASA TM X-2894, 1974.

11. Beckwith, I. E.: "Comments on Crocco's Solution and Independence Principle for Compressible Turbulent Boundary Layers." AIAA Journal, Vol. 7, No. 3, March 1969.

12. Beckwith, I. E.: "Development of High Reynolds Number Quiet Tunnel for Transition Research." AIAA Paper 74-135, AIAA 12th Aerospace Sciences Meeting, January 30-February 1, 1974.

13. Stainback, P. C.; Anders, J. B., Jr.; Harvey, W. D.; Cary, A. M., Jr.; and Harris, J. E.: "An Investigation of Boundary Layer Transition on the Wall of a Mach 5 Nozzle," Parts I and II. AIAA Paper 74-136, AIAA 12th Aerospace Sciences Meeting, January 30-February 1, 1974.

14. Pfenninger, W.; and Syberg, J.: "Reduction of Acoustic Disturbances in the Test Section of Supersonic Wind Tunnels by Laminarizating Their Nozzle and Test Section Wall Boundary Layers by Means of Suction." NASA CR-2436, March 1974.

15. Groth, E. E.; Pate, S. R.; and Nenni, J. P.: "Laminar Flow Control at Supersonic Speeds." Recent Developments in Boundary Layer Research, Part IV, AGARDOgraph 97, May 1965.

16. Beckwith, I. E.; and Bertram, M. H.: "A Survey of NASA Langley Studies on High Speed Transition and the Quiet Tunnel." NASA TM X-2566, July 1972.

17. Harvey, W. D.; Berger, M. H.; and Stainback, P. C.: "Experimental and Theoretical Investigation of a Slotted Noise Shield Model for Wind Tunnel Walls." AIAA Paper 74-624, AIAA 8th Aerodynamic Testing Conference, Bethesda, Maryland, July 8-12, 1974.

18. Binion, T. W., Jr.; and Anderson, C. F.: "An Experimental Investigation of the Acoustic and Wall Interference Properties of Rod and Perforated Wind Tunnel Walls in Two-Dimensional Transonic Flow." AEDC-TR-74-41, September 1974.

19. Harvey, William D.: "Effects of Leading-Edge Bluntness on Pressure and Heat-Transfer Measurements Over a Flat Plate at a Mach Number of 20." NASA TN D-2846, October 1964.

20. Berger, M. H.: "Application of Boundary Layer Theory to Suction Through Streamwise Slots in Wind Tunnel Walls." M.S. Thesis, Old Dominion University, Norfolk, Virginia, June 1974.

21. Hixon, B. A.; Beckwith, I. E.; and Bushnell, D. M.: "Computer Program for Compressible Laminar or Turbulent Nonsimilar Boundary Layers." NASA TM X-2140, April 1971.

22. Sayano, S.; and Greenwald, G. F.: "Approximate Method for Calculating Heat Transfer to Yawed Cylinders in Laminar Flow." Journal of Spacecraft and Rockets, February 1973, pp. 157-159.

23. Cary, A. M., Jr.; and Morrisette, E. L.: "Effect of Two-Dimensional Multiple Sine-Wave Protrusions on the Pressure and Heat-Transfer Distributions for a Flat Plate at Mach 6." NASA TN D-4437, March 1968.

24. Bushnell, D. M.: "Effects of Shock Impingement and Other Factors on Leading-Edge Heat Transfer." NASA TN D-4543, April 1968.

25. Bushnell, D. M.: NASA Langley, Hampton, Virginia, Private Communication, 1973.

26. Bushnell, D. M.; and Huffman, J. K.: "Investigation of Heat Transfer to Leading Edge of a 76° Swept Fin With and Without Chordwise Slots and Correlations of Swept-Leading-Edge Transition Data for Mach 2 to 8." NASA TM X-1475.

27. Burbank, P. B.; Newlander, R. A.; and Collins, I. R.: "Heat-Transfer and Pressure Measurements on a Flat-Plate Surface and Heat Transfer Measurements on Attached Protuberances in a Supersonic Turbulent Boundary Layer at Mach Numbers of 2.65, 3.51, and 4.44." NASA TN D-1372, December 1962.

28. Rao, D. M.; and Whitehead, A. H., Jr.: "Lee-Side Vortices on Delta Wings at Hypersonic Speeds." AIAA Journal, Vol. 10, No. 11, November 1972, pp. 1458-1465.

29. Whitehead, A. H., Jr.; Hefner, J. N.; and Rao, D. M.: "Lee-Surface Vortex Effects Over Configurations in Hypersonic Flow." Presented at AIAA 10th Aerospace Sciences Meeting, San Diego, California, January 17-19, 1972.

30. Laufer, J.: "Aerodynamic Noise in Supersonic Wind Tunnels." Journal of the Aeronautical Sciences, Vol. 28, 1961, pp. 685-692.

31. Goldberg, T. J.; and Hefner, J. N.: "Starting Phenomena for Hypersonic Inlets With Thick Turbulent Boundary Layers at Mach 6." NASA TN D-6280, August 1971.

32. Beckwith, I. E.; Srokowski, A. J.; Harvey, W. D.; and Stainback, P. C.: "Design and Preliminary Test Results at Mach 5 of an Axisymmetric Slotted Sound Shield." NASA TM X-72679, March 1975.

33. Beckwith, I. E.; Harvey, W. D.; Harris, J. E.; and Holley, B. B.: "Control of Supersonic Wind Tunnel Noise by Laminarization of Nozzle Wall Boundary Layers." NASA TM X-2879, 1973.